X-ray Analysis of Fully Depleted Thick CCDs with Small Pixel Size

Ivan Kotov
Brookhaven National Laboratory

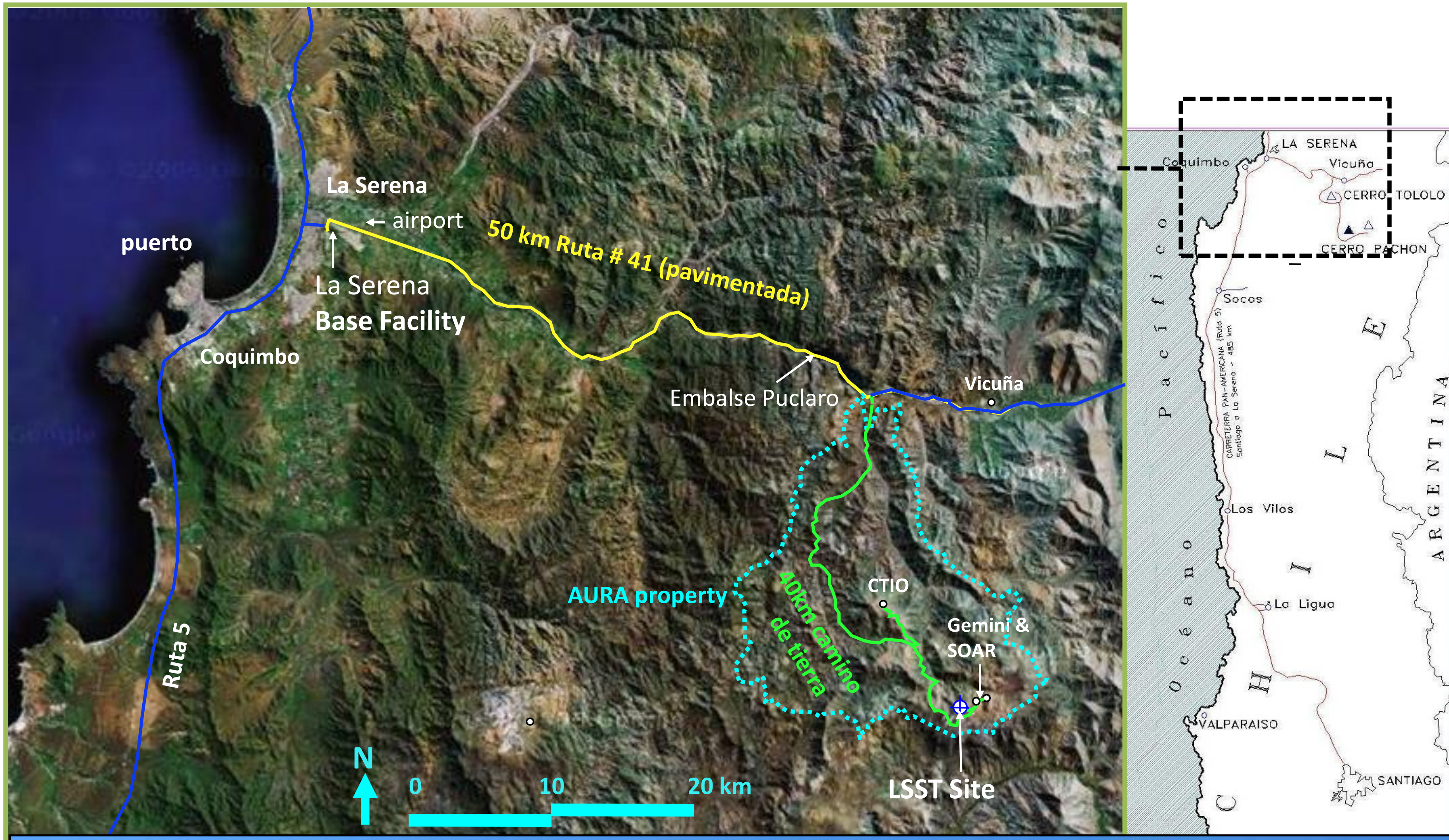
La Serena
airport
50 km Ruta # 41 (pavimentada)
puerto
La Serena
Base Facility
Coquimbo
Embalse Puclaro
Vicuña
AURA property
40km camino de tierra
CTIO
Gemini & SOAR
Ruta 5
N
0
10
20 km
LSST Site
LA SERENA
Coquimbo
Vicuña
CERRO TOLOLO
CERRO PACHON
Socos
Los Vilos
La Ligua
VALPARAISO
SANTIAGO
Océano Pacífico
CHILE
ARGENTINA

er

Telescope, Camera, etc

Relevant Telescope Features
3 mirror optical design
Moving structure: 300 tons
Altitude/azimuth rotation axes
Camera is cantilevered off the Top End Assembly near the center of rotation
Camera normally looks down when telescope is pointing near zenith

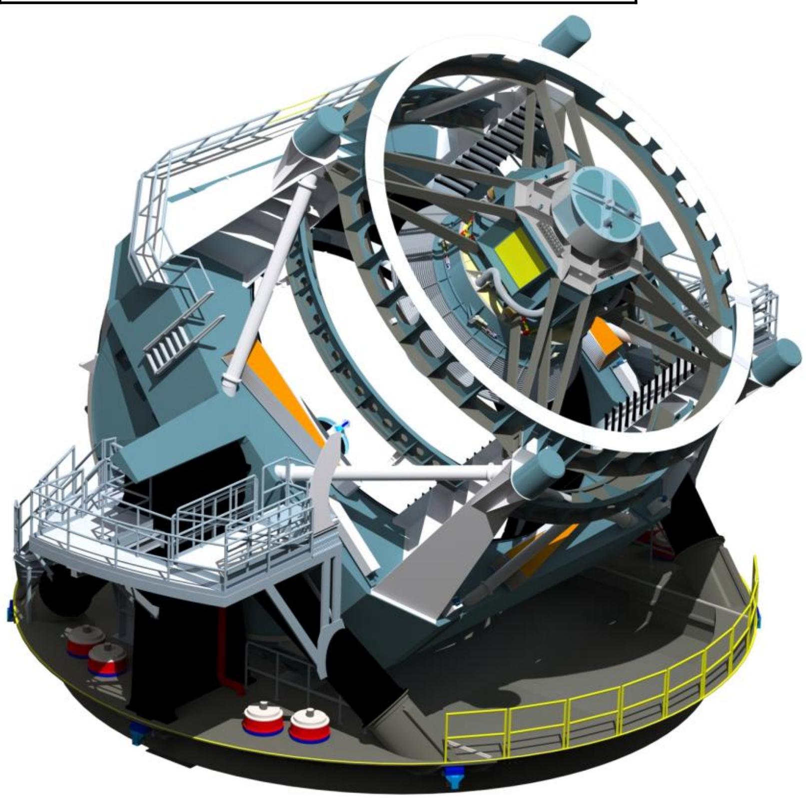

NSF: Telescope and Site Preparation

+

U.S. DEPARTMENT OF ENERGY: Camera, Shutter, Filters, Corrector

NSF: Image Analysis Software
Database Implementation

Multiple Science Goals from Same Image Stream

The LSST Focal Plane - 64 cm in Diameter

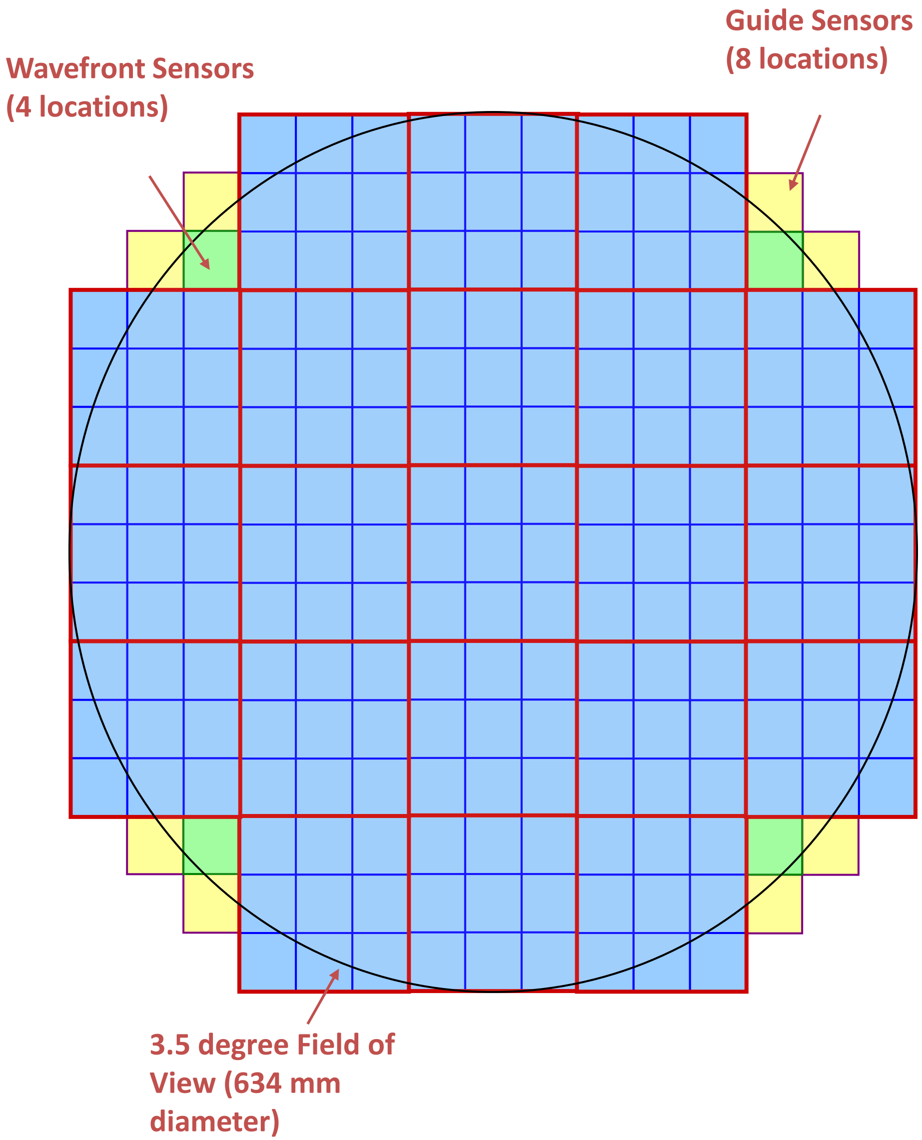

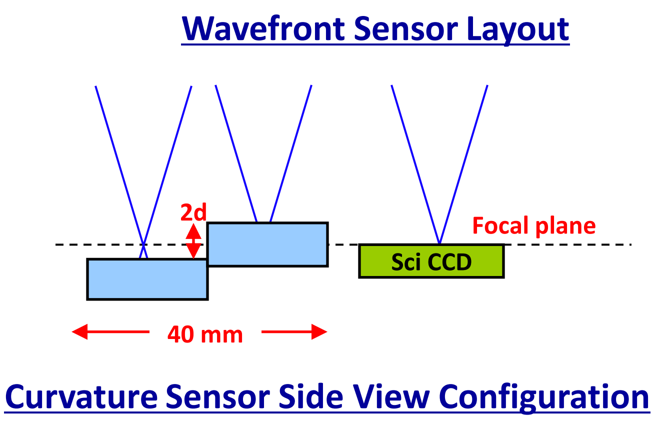

CCD Sensor

16 segments/CCD
200 CCDs total
3200 Total Outputs

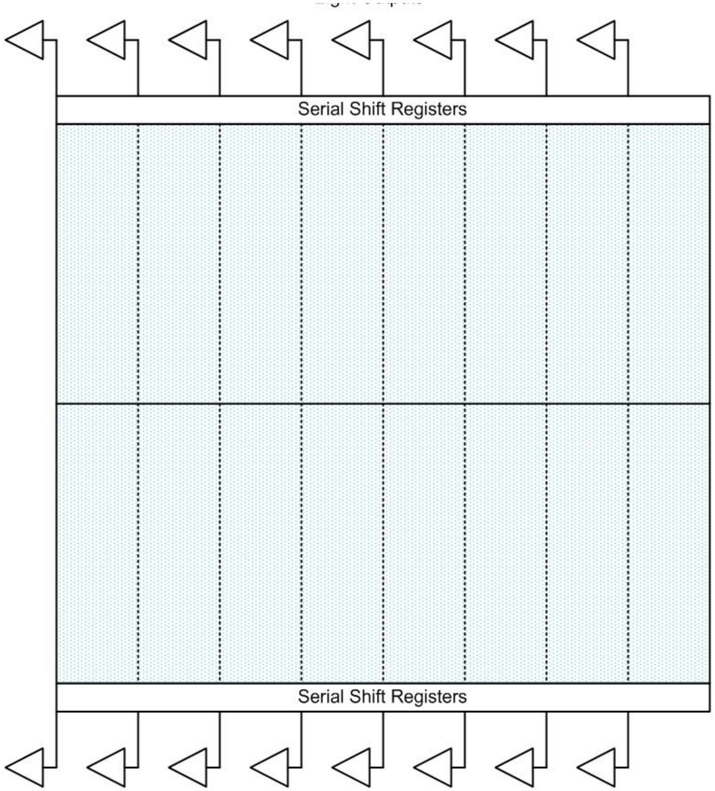

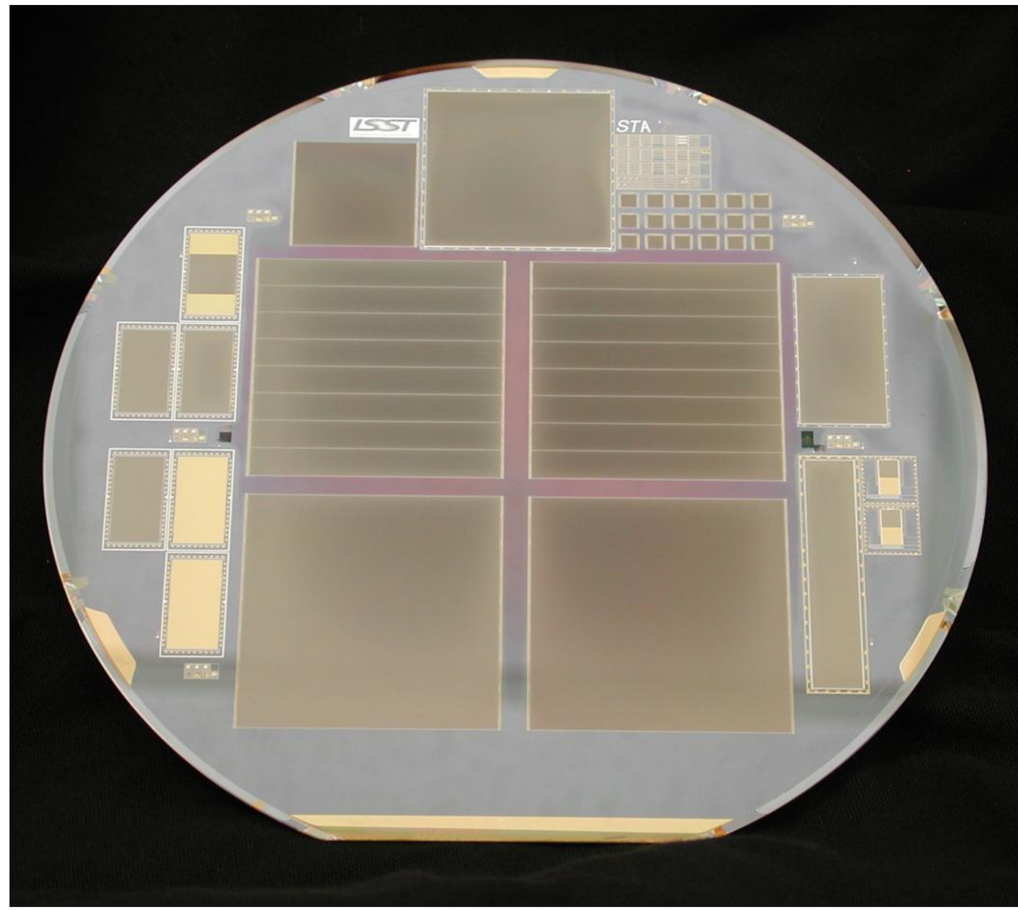

Sensor Characterization

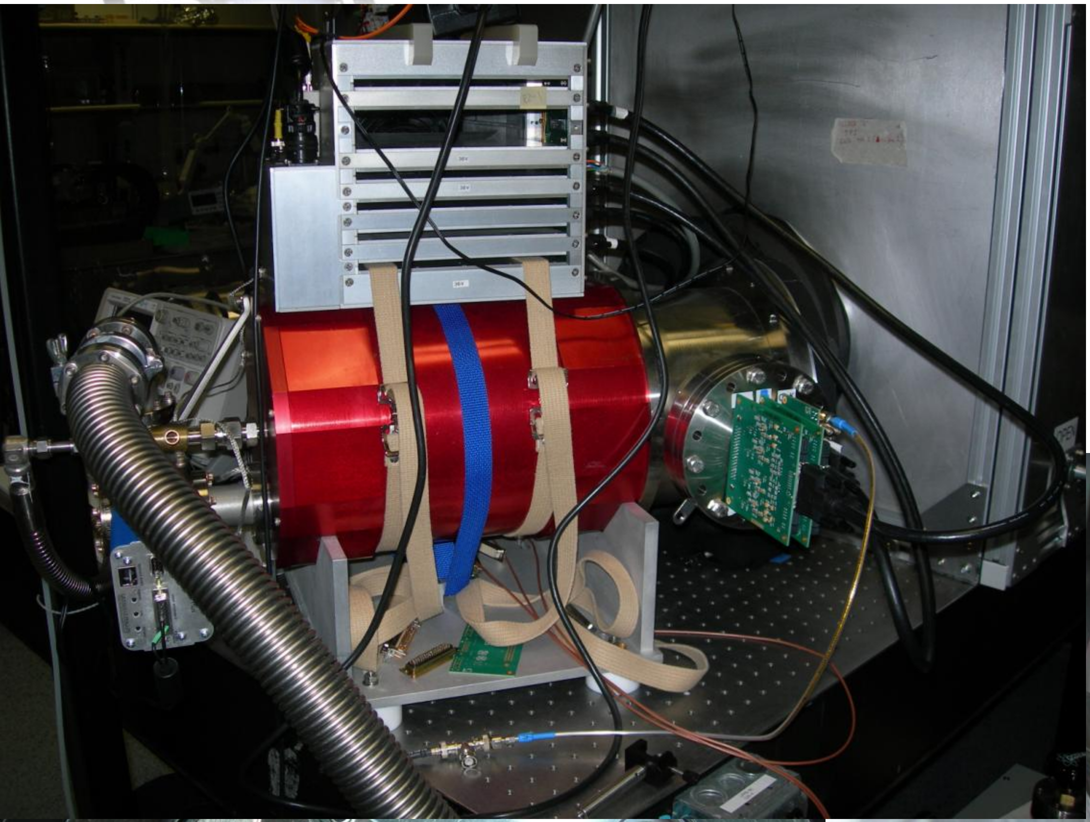

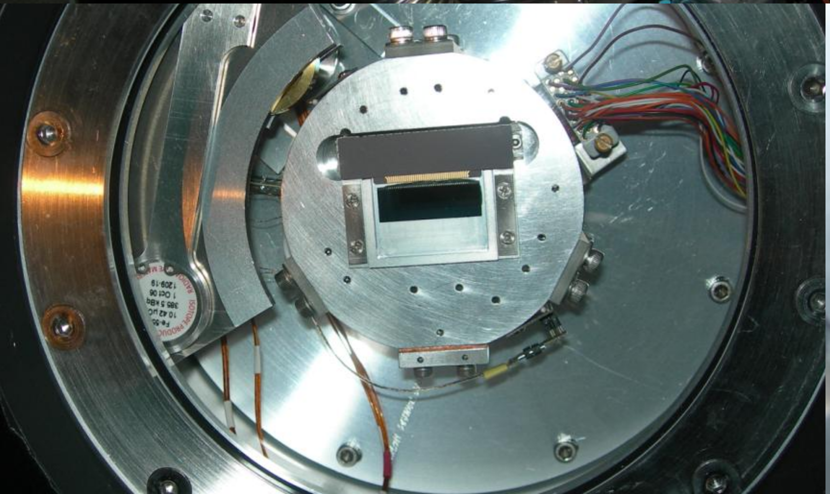

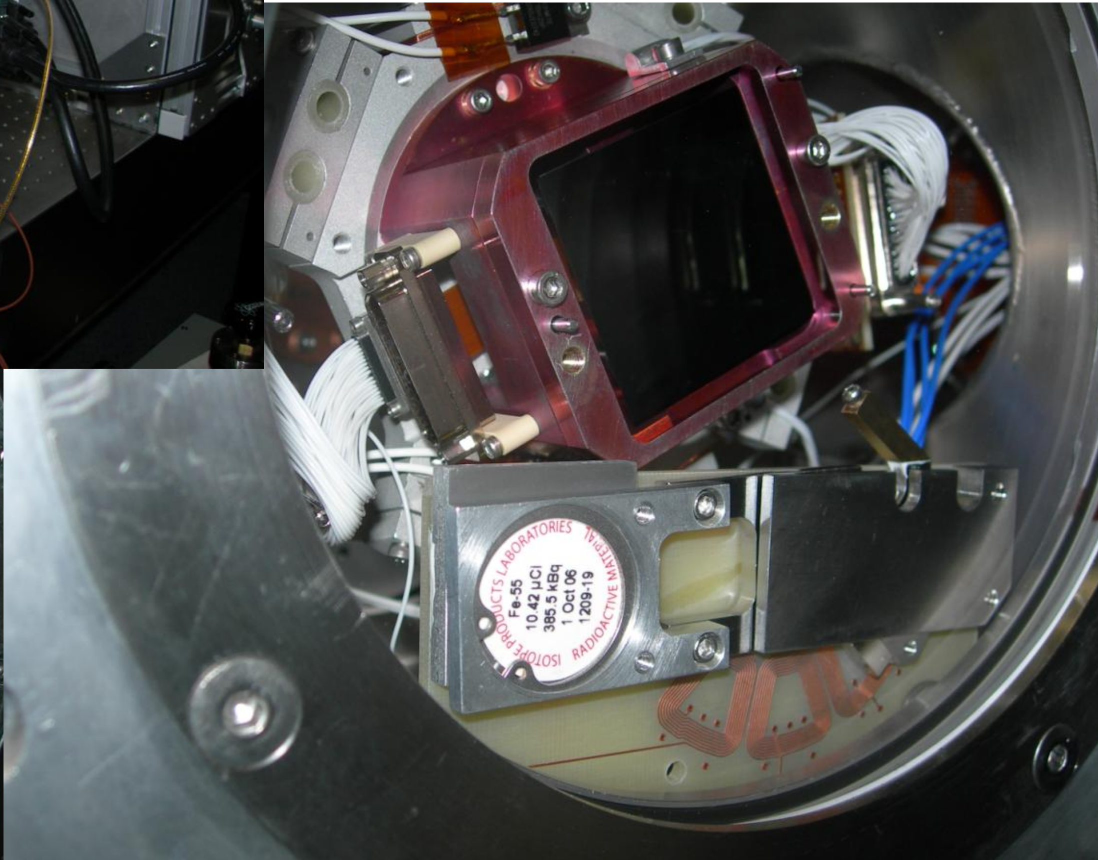

^{55}Fe data, segment 2

- Noise: 6.5e-
- ~1,000,000 ^{55}Fe $K_{\alpha,\beta}$ clusters
- 99% are clusters with 4 or more "fired" pixels > 1.2 σ_{noise}

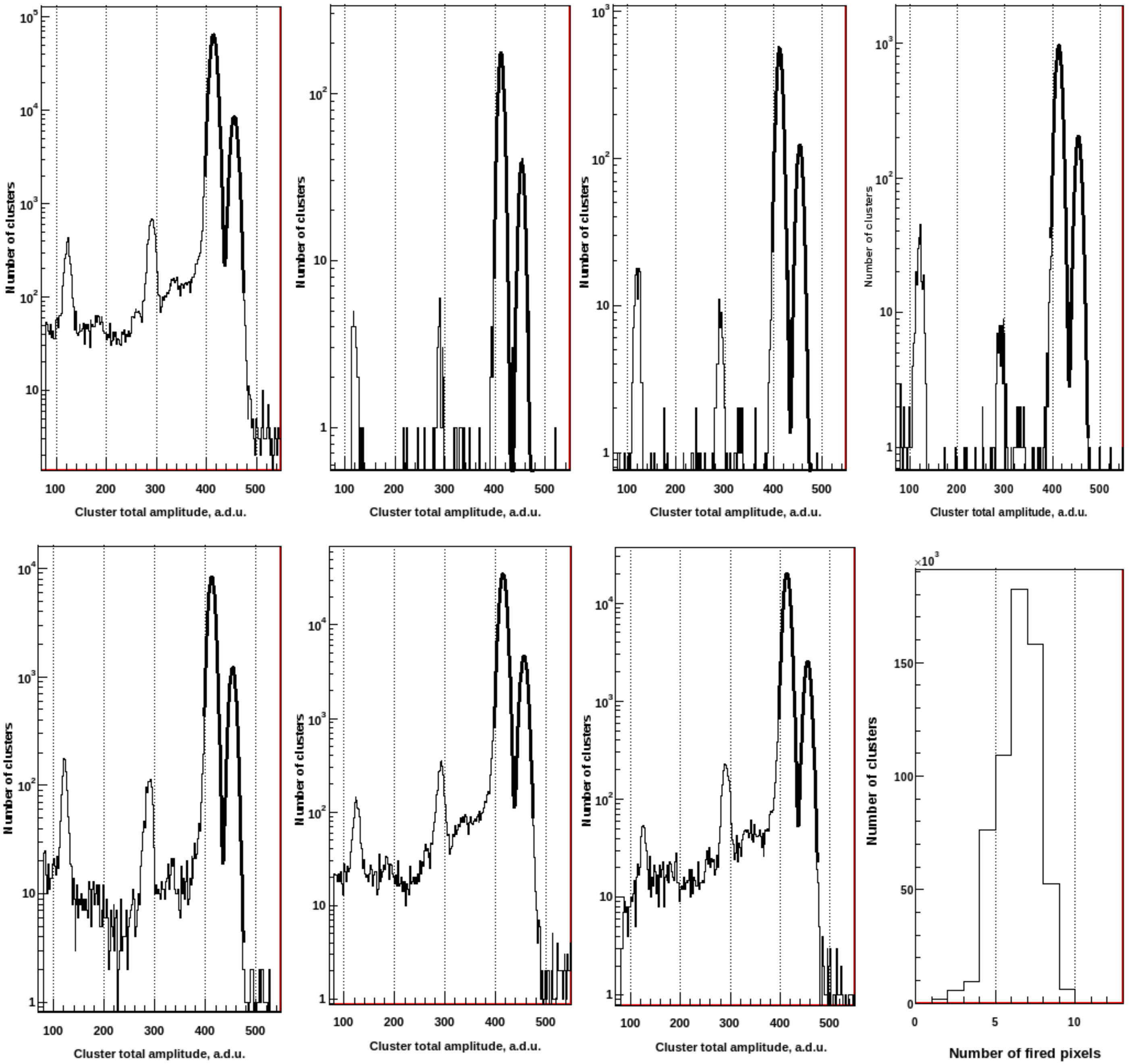

^{55}Fe spectra

^{55}Fe → electron capture → ^{55}Mn

X-rays from ^{55}Fe (2.73 y *3*)

E (keV)	I (%)	Assignment	
5.770	6.9E-06 *4*	Mn $K_{\alpha 3}$	K_α 25.4%
5.888	8.5 *4*	Mn $K_{\alpha 2}$	
5.899	16.9 *8*	Mn $K_{\alpha 1}$	
6.490	1.01 *5*	Mn $K_{\beta 3}$	K_β 3%
6.490	1.98 *10*	Mn $K_{\beta 1}$	
6.536	0.00089 *5*	Mn $K_{\beta 5}$	
6.539	8.5E-08 *5*	Mn $K_{\beta 4}$	

5.19 Auger e- 60%

Si	$K\alpha_2$	$K\alpha_1$	$K_{\beta 1}$
	1.739394(34)	1.739985(19)	1.836
	0.593	0.296	0.111

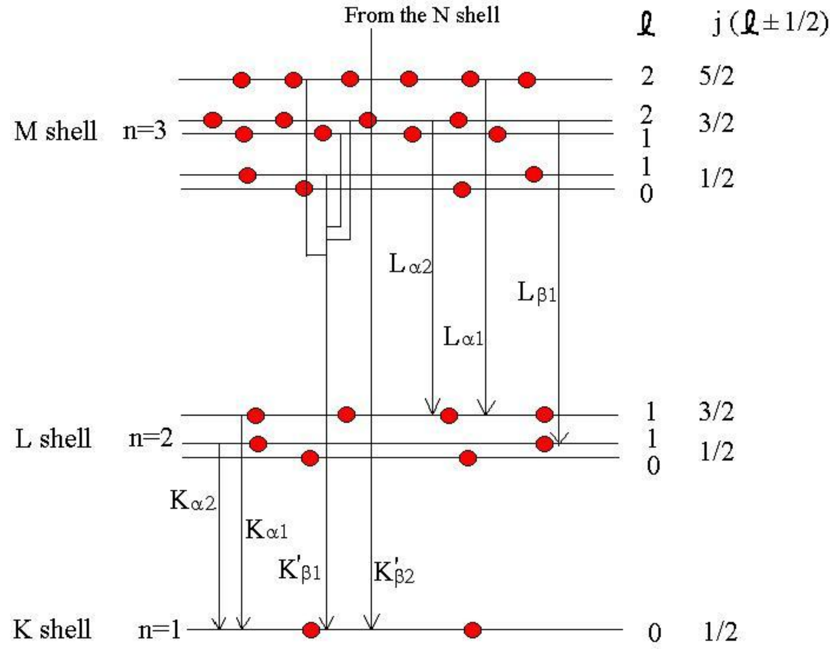

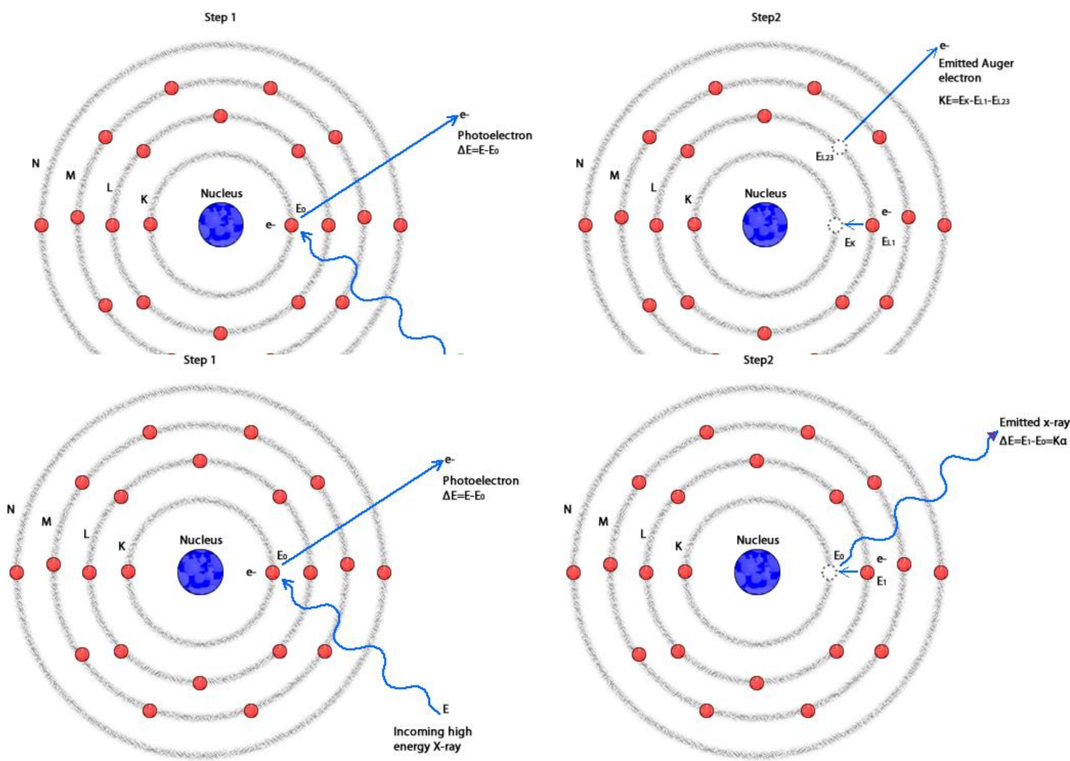

^{55}Fe spectra, fit, fit, fit..

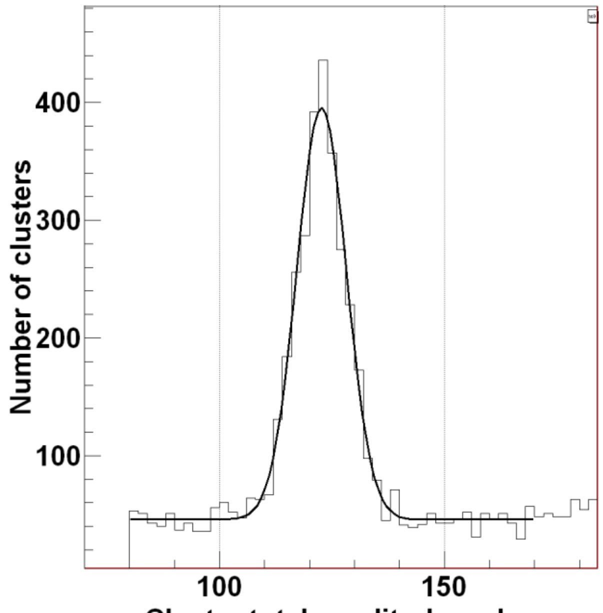

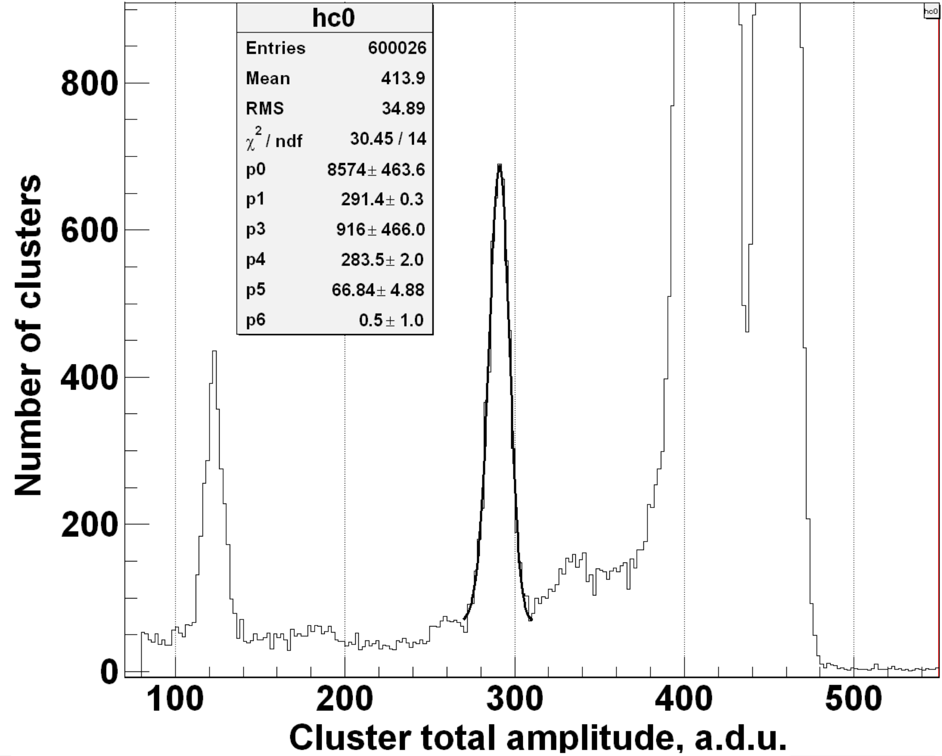

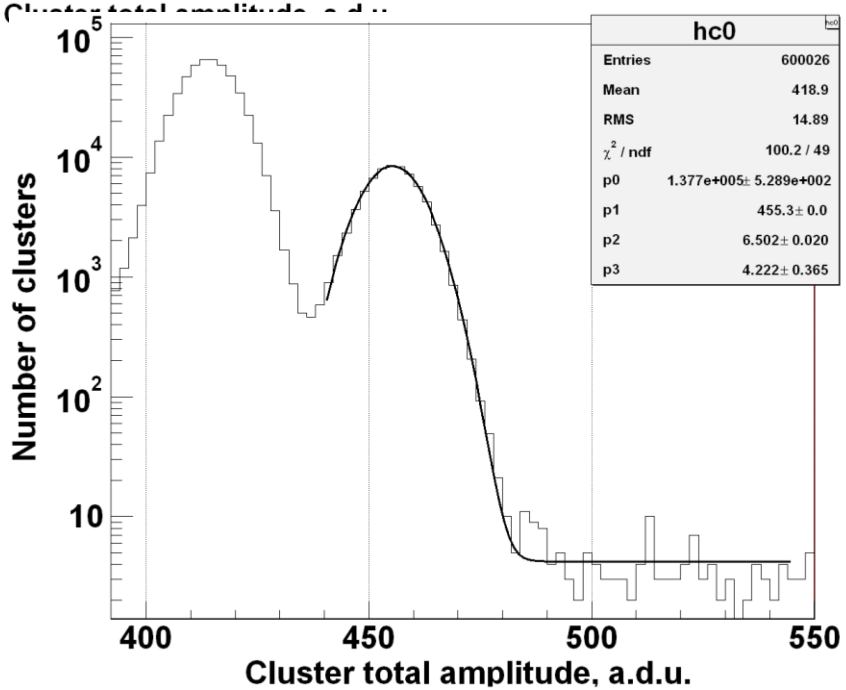

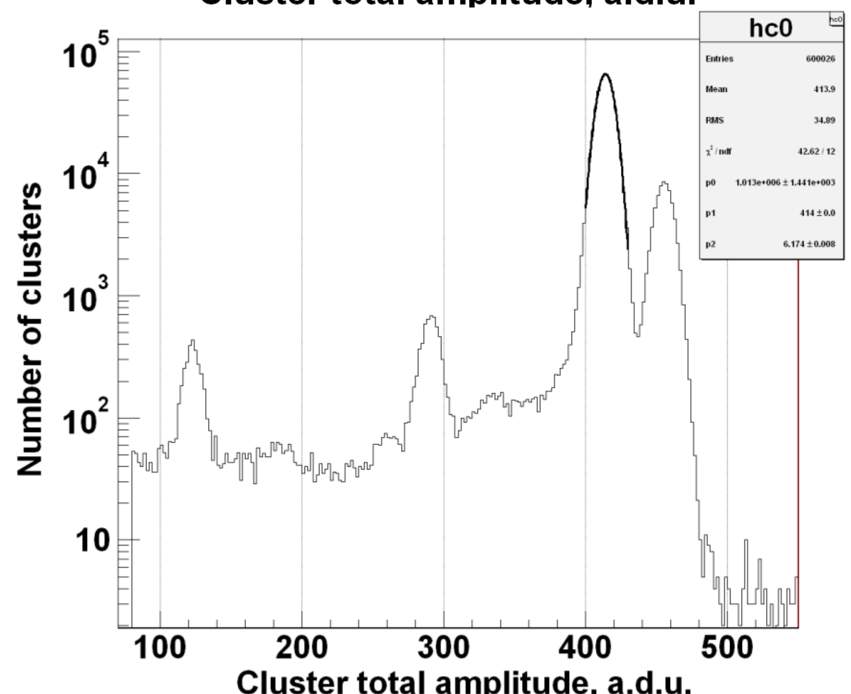

^{55}Fe spectra summary

Line	Relative probality	Energy, keV	Pairs created, 3.68eV/pair	Line width (FF=0.11), e-	Peak position, adu	Conversion gain, e-/adu	# events
Mn K_β	120,000	6.490	1763.6	13.9	455.26+/-0.03	3.874	137,700
Mn K_α	1,000,000	5.895	1601.9	13.3	413.98+/-0.01	3.870	1,013,420
Mn K_β escα	4,700	4.750	1290.8	11.9			
Mn K_β escβ	580	4.654	1264.7	11.8			
Mn K_α escα	39,000	4.155	1129.1	11.1	291.4+/-0.3	3.875	8600
Mn K_α escβ	4,800	4.059	1103.0	11.0			920
Si K_β	5,000	1.836	498.9	7.4			
Si K_α	44,000	1.740	472.8	7.2	122.7+/-0.14	3.875	4800

3.873 +/- 0.1%

^{55}Fe spectra, line width summary

Pairs created, 3.68eV/pair	Line width (FF=0.11), e-	Peak position, adu	Peak σ, adu	Noise per pixel, e-
1763.6	13.9	455.26+/-0.03	6.50+/-0.02	6.99
1601.9	13.3	413.98+/-0.01	6.13+/-0.01	6.55
1129.1	11.1	291.4+/- 0.3	6.07+/-0.1	6.91
472.8	7.2	122.7+/-0.14	5.5+/-0.1	6.68

^{55}Fe data, all segments

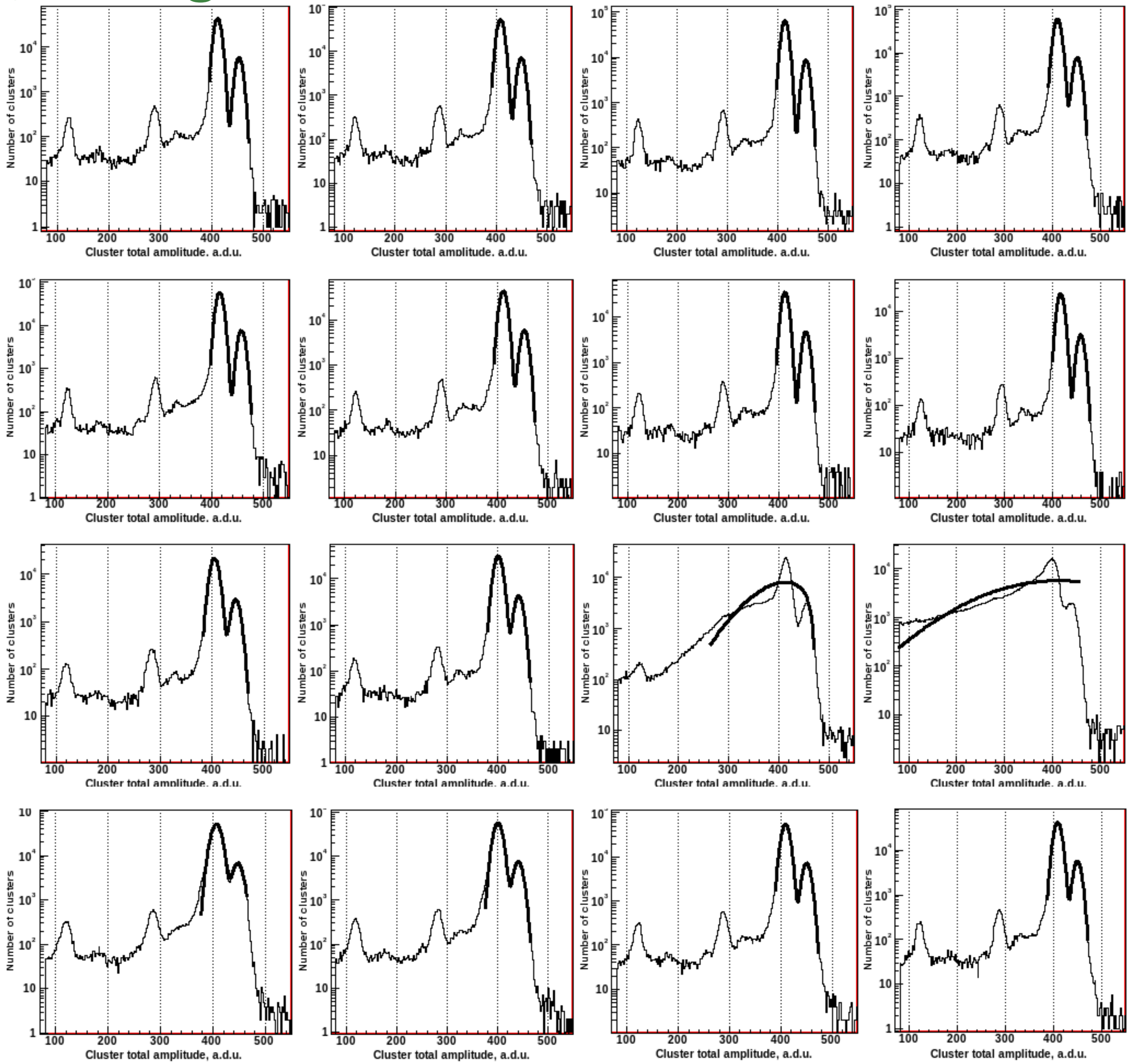

Sensor Point Spread Function = Diffusion

- Charge diffusion measurements
- charge carrier transport from the back window to the gates is accompanied by charge diffusion. Expected value: "Charge Diffusion PSF in Thick Over-depleted Silicon Sensors ", Veljko Radeka, Zheng Li, Paul O'Connor, Peter Takacs, ICSOI, Cozumel, Mexico 2006 →

  .. in the range of ***3-3.5*** μm @173K and electric field of ~5kV/cm..

  → value of interest is diffusion sigma for charges generated on the surface
  - the charge distribution has a 2D Gaussian shape
  - numerous methods have been developed and we've tried them for lateral diffusion characterization, VKE, MTF, cosmic ray tracks etc
    - they all have their own sources of systematic uncertainties
- ^{55}Fe X-rays
  - it is very attractive to use ^{55}Fe data for charge diffusion characterization
  - conversion happens at all depths but
    - the number of X-rays converted near the window is about 30 times higher than near the gates
    - the distribution of sigma values in a ^{55}Fe sample has a peak at the "window" value

Diffusion measurements: the new method

- the 2D Gaussian charge distribution can be described by 4 parameters:
  - conversion point x- and y-position
  - total amplitude
  - diffusion sigma

- 4 parameters can be determined for an individual X-ray cluster if cluster contains at least 4 pixels with amplitudes above the noise (2D fit)

- the low CCD noise enable the measurement of small diffusion sigma even though the pixel size is large (2-3 times larger than sigma value)

Data & Simple Simulations

- Measurements and simulation are in good agreement (for the ``window'' peak).
- The characteristic diffusion value for these measurements is estimated as sigma = 3.6 micron.
- The statistical accuracy can be estimated using the r.m.s. of the blue histogram as ~0.01micron.
- More extensive simulations are shown bellow.

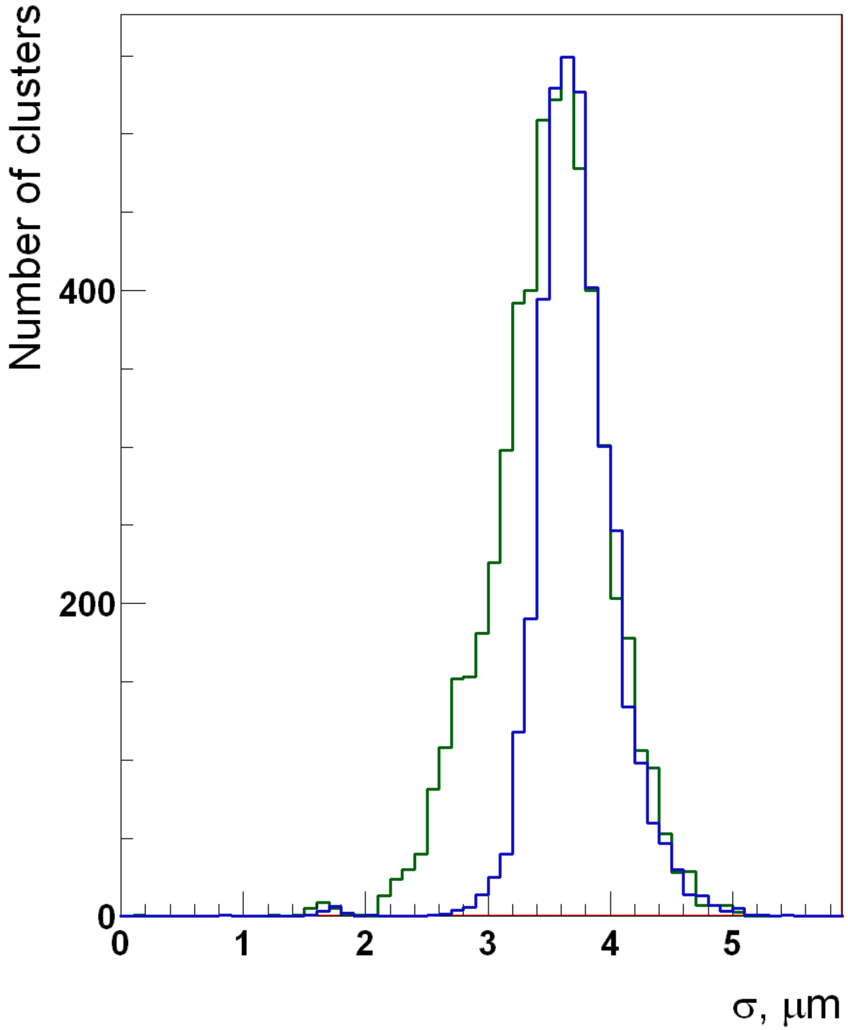

Data & Full Simulations

- Measurements and simulation are in good agreement.
- The max characteristic diffusion value for these simulations is sigma = 3.65 micron.
- Systematic uncertainties are related to model parameters, geometry, noise etc.

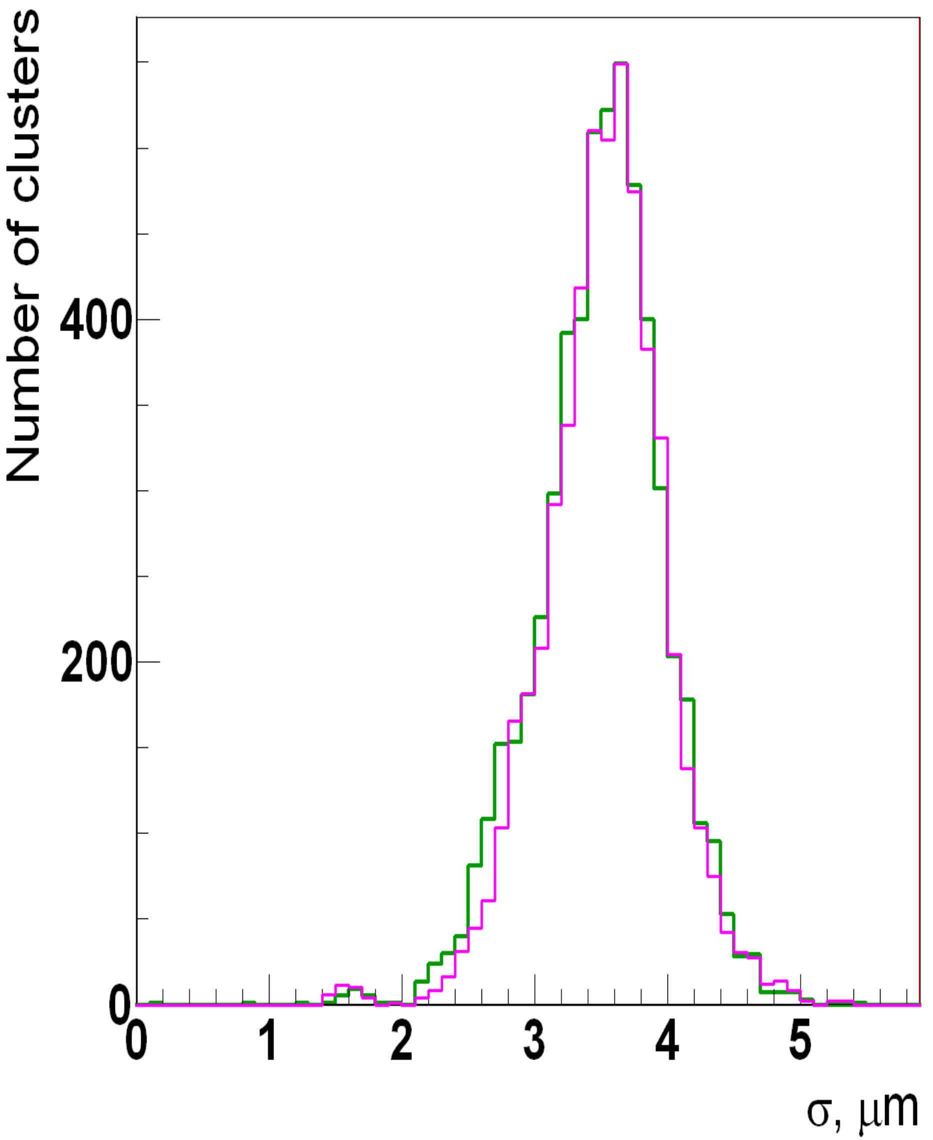

High Stat Data

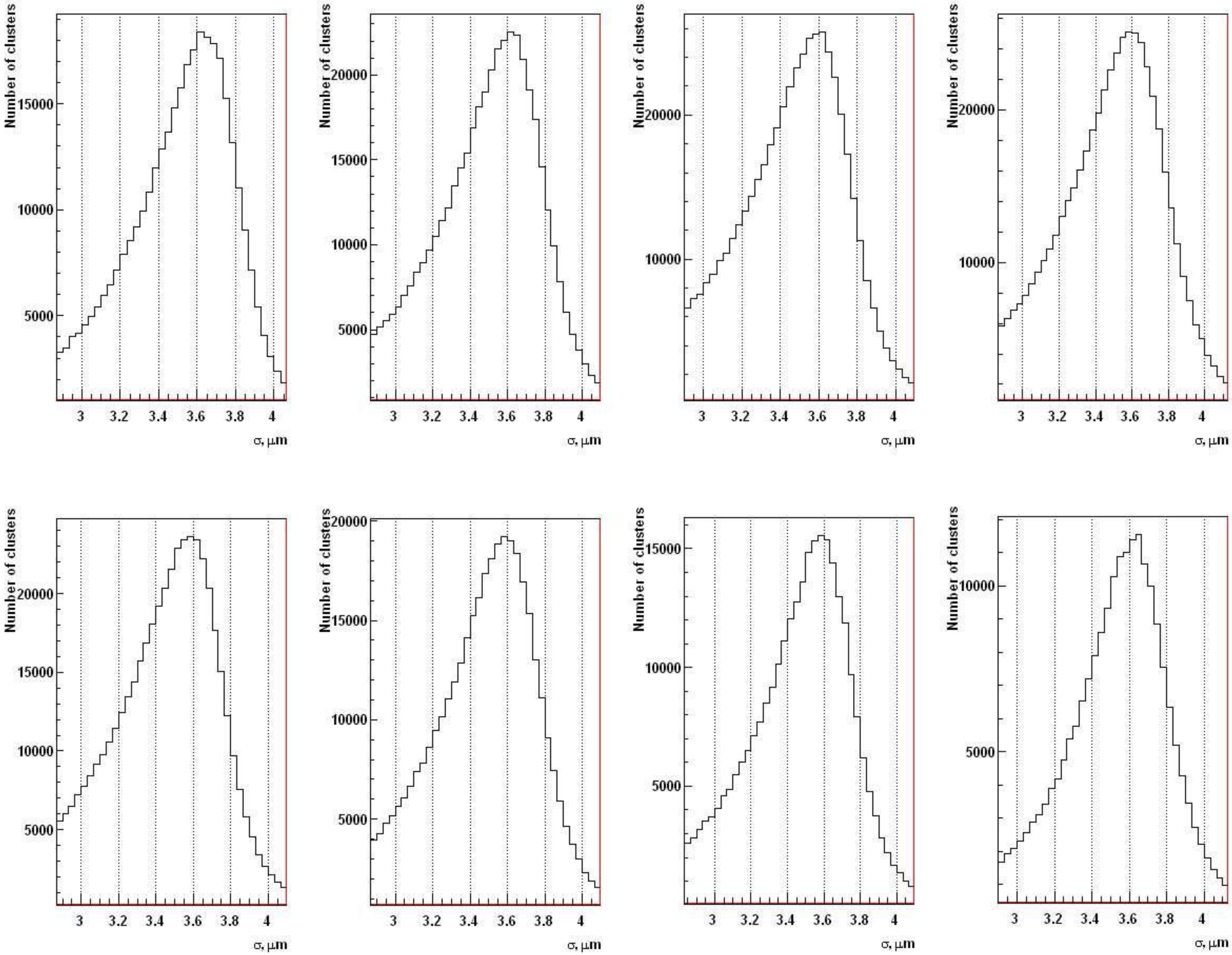

K_α Average Hit

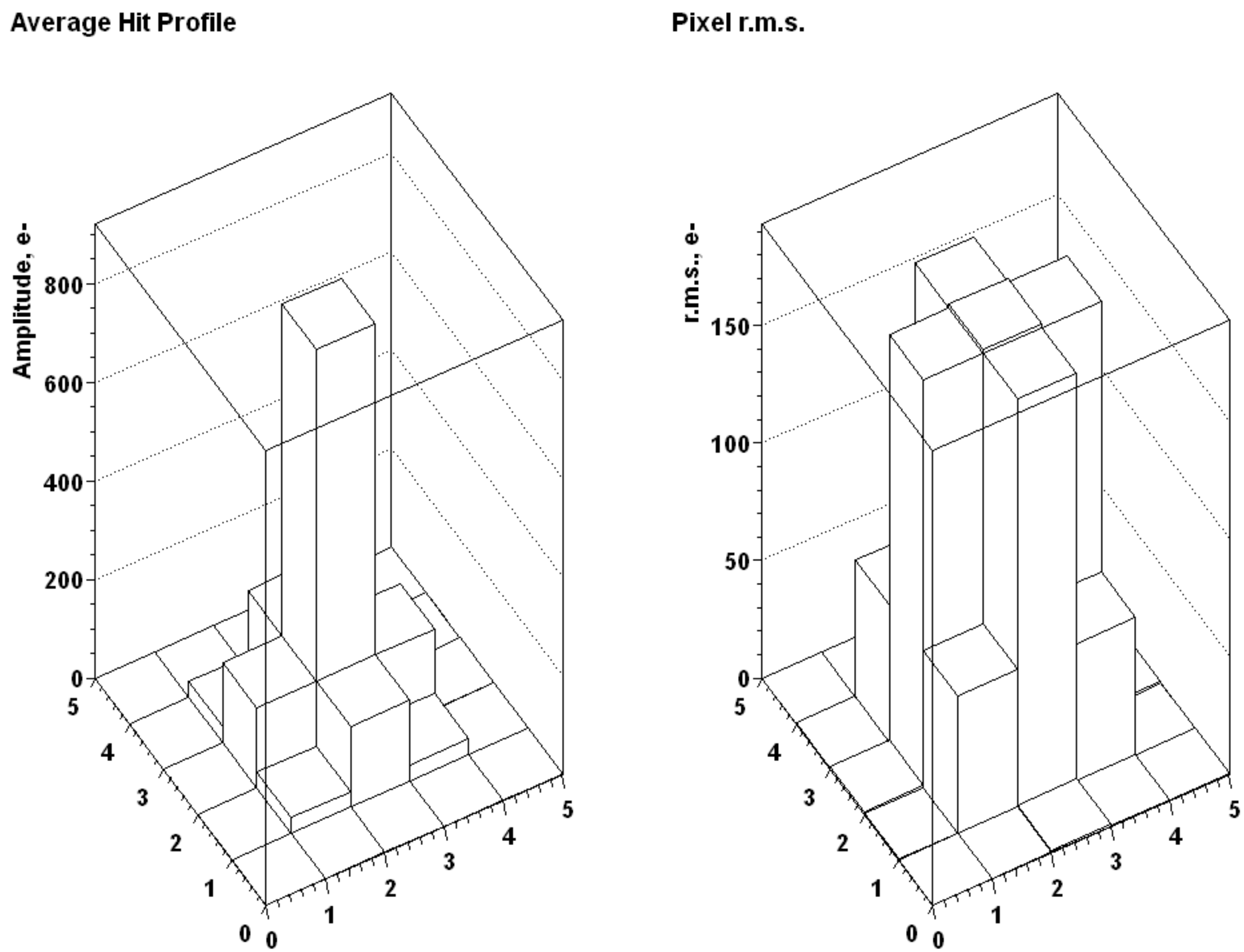

- analytical
- K_α cluster
- conversion points are anywhere within the center pixel

CCD Readout Architecture Terms

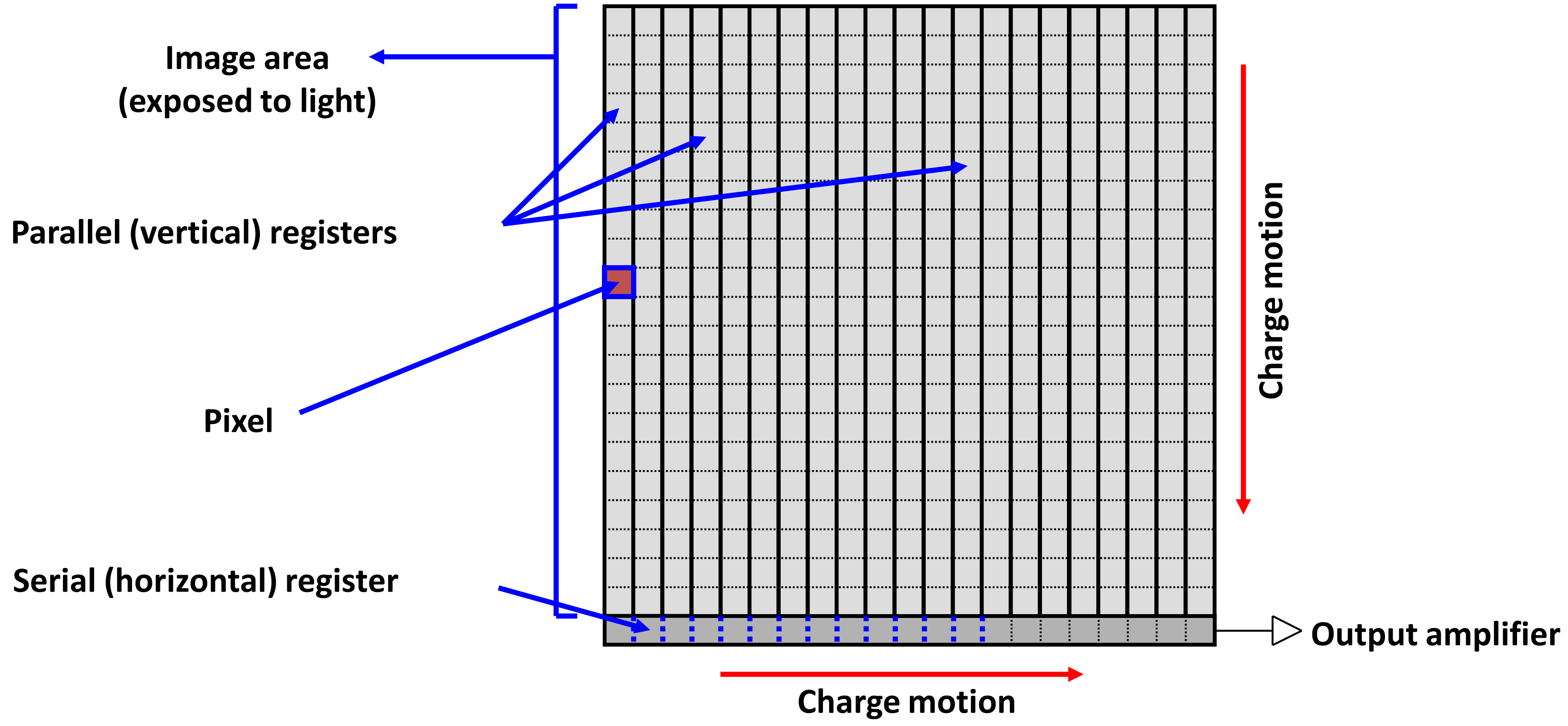

CCD Phased Clocking: Step 1

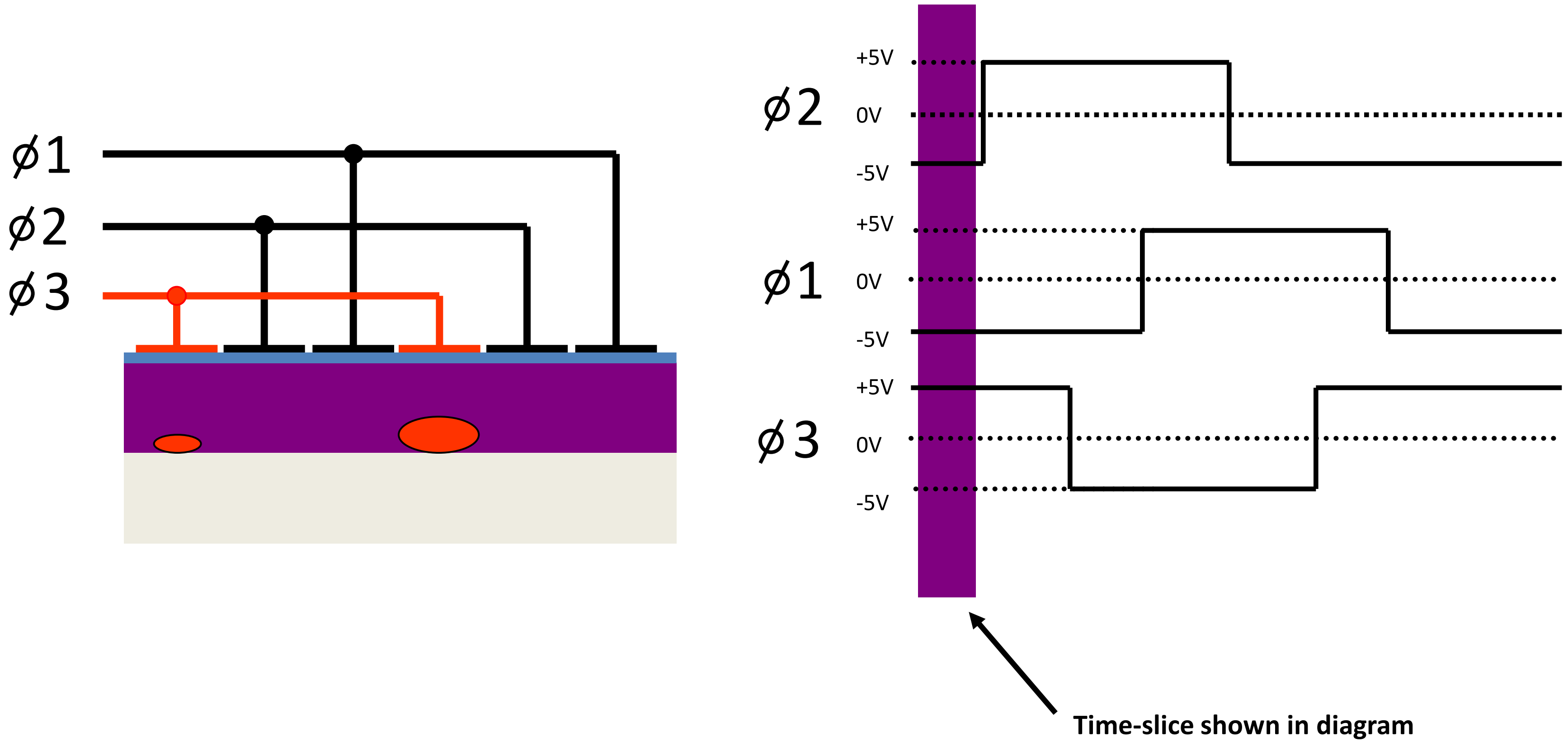

CCD Phased Clocking: Step 2

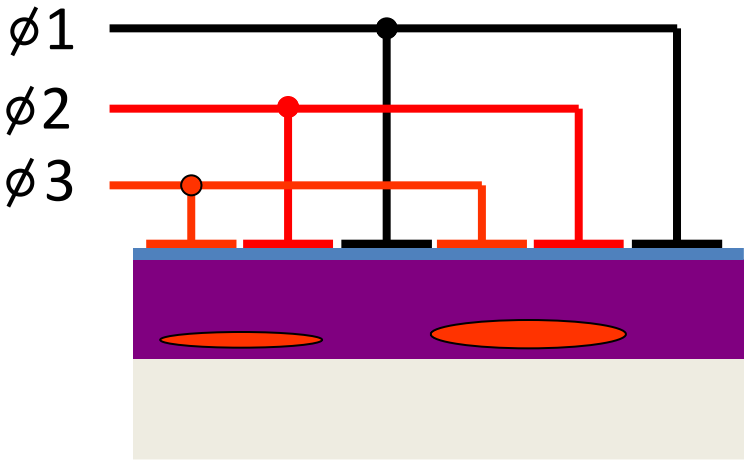

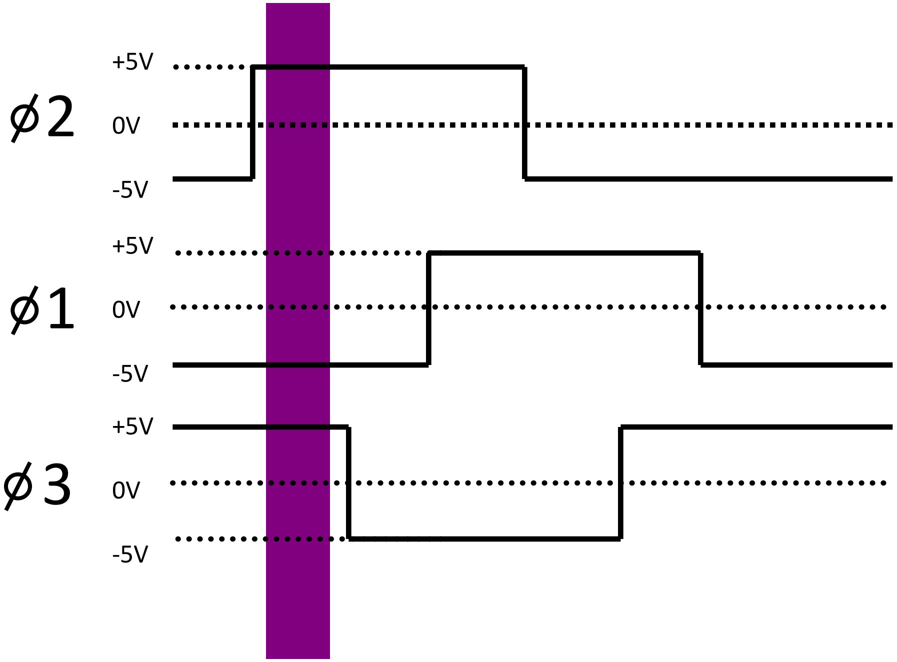

CCD Phased Clocking: Step 3

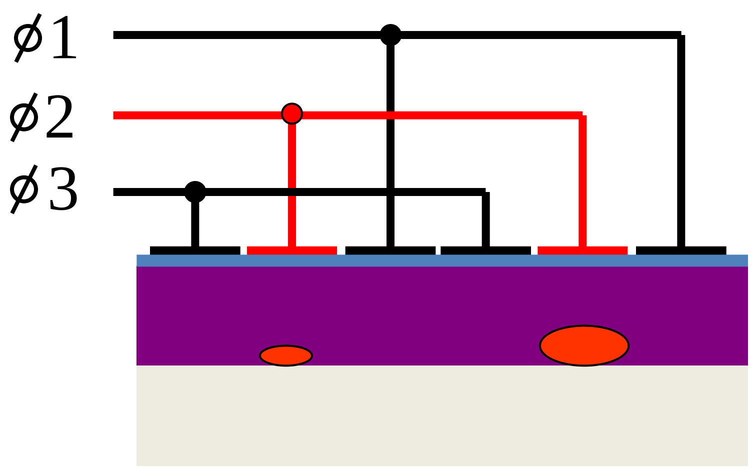

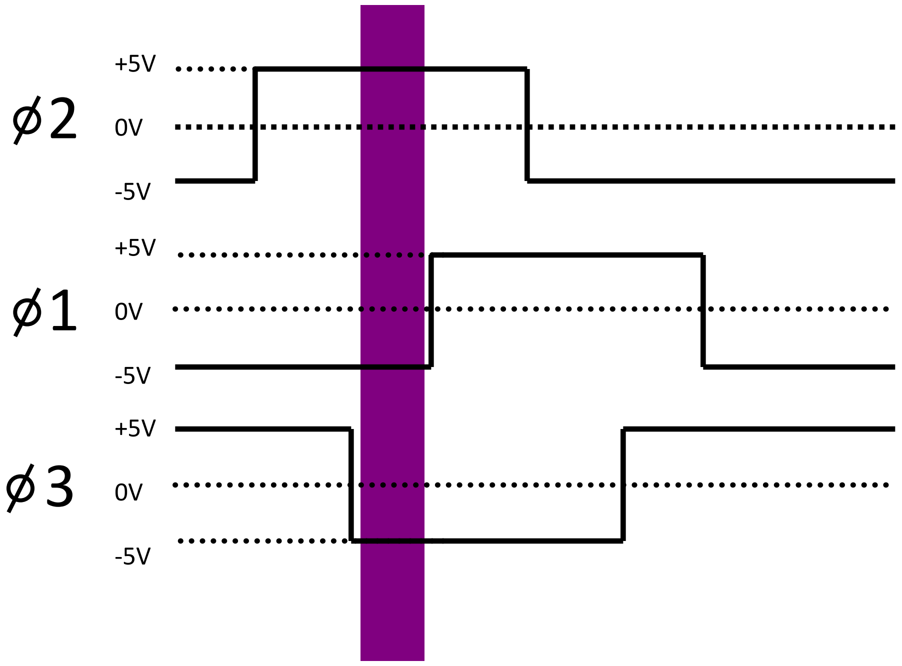

Charge Transfer Efficiency

CTE = Charge Transfer Efficiency (typically 0.9999 to 0.999999)
= fraction of electrons transferred from one pixel to the next

CTI = Charge Transfer Inefficiency = 1 – CTE (typically 10^{-6} to 10^{-4})
= fraction of electrons deferred by one pixel or more

Cause of CTI:
charges are trapped (and later released) by defects in the silicon crystal lattice

CTE of 0.99999 used to be thought of as pretty good but ….

Think of a 2K x 0.5K CCD segment

CTE measurements with X-rays

3x3 zone is the minimal region containing

- 99.9% or more energy on average
- 99.5% energy always

Using this zone to measure X-ray energy is an example of aperture photometry application.
CTE measured using total amplitude in this zone is arguably a
good quantity to describe the charge loss in CCD readout process.

In normal operational conditions, T=-100C CTE is better than **0.999999**
in both serial and parallel directions.

CTE degradation is observed at T=-150C
serial CTE = **0.999928** (CTI = 7.2x10-5)
parallel CTE better than 0.999999

CTE measurements with X-rays. Normal conditions

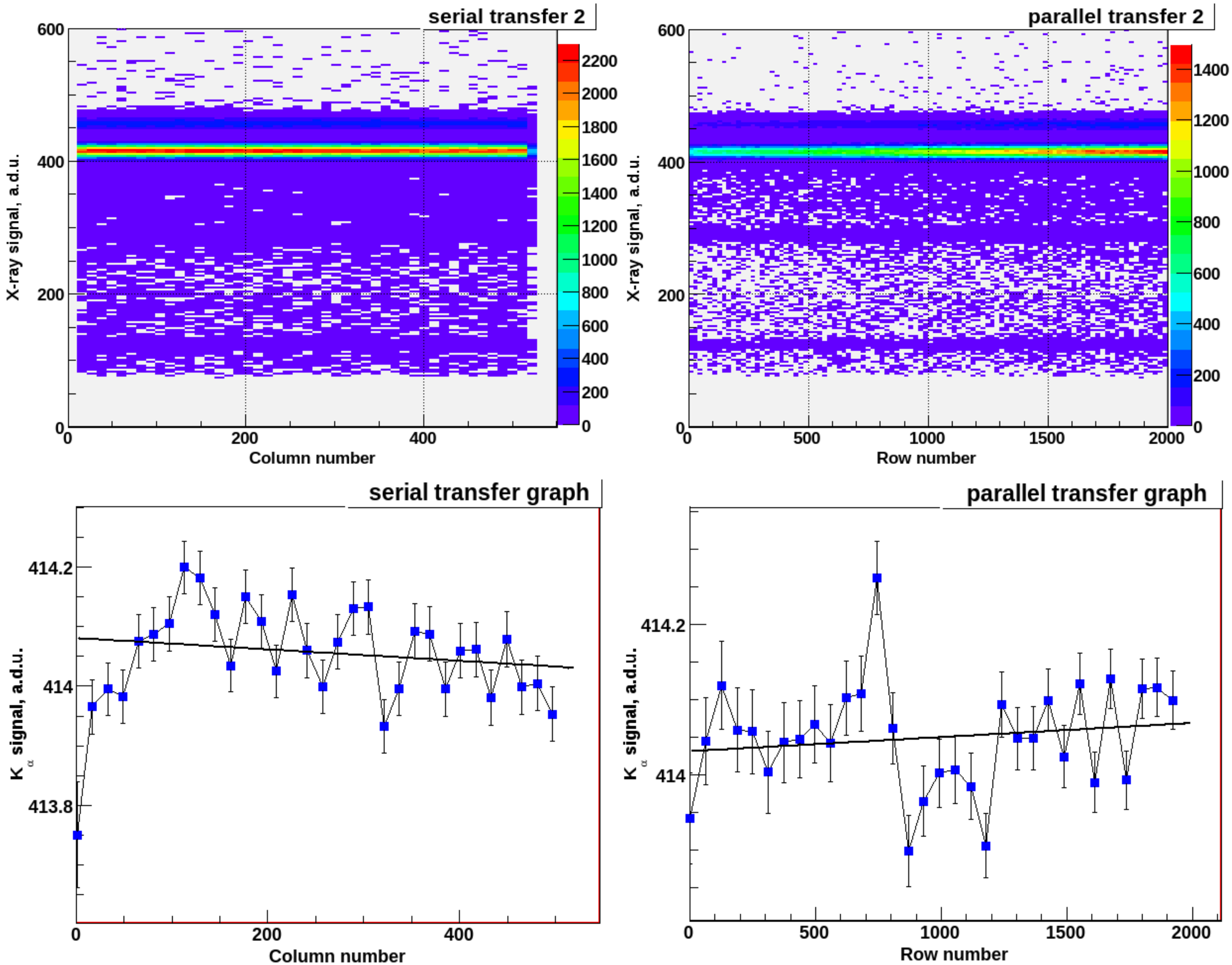

CTE measurements with X-rays. T=-150C

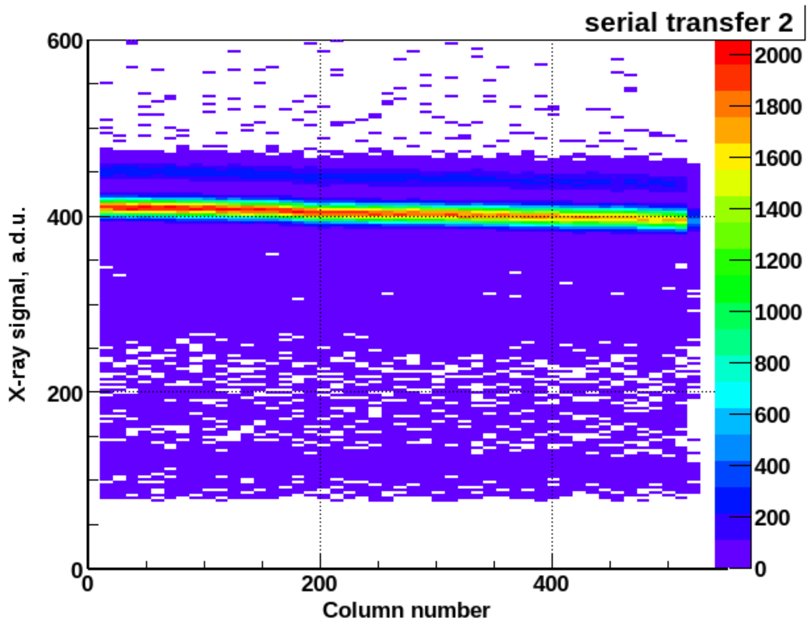

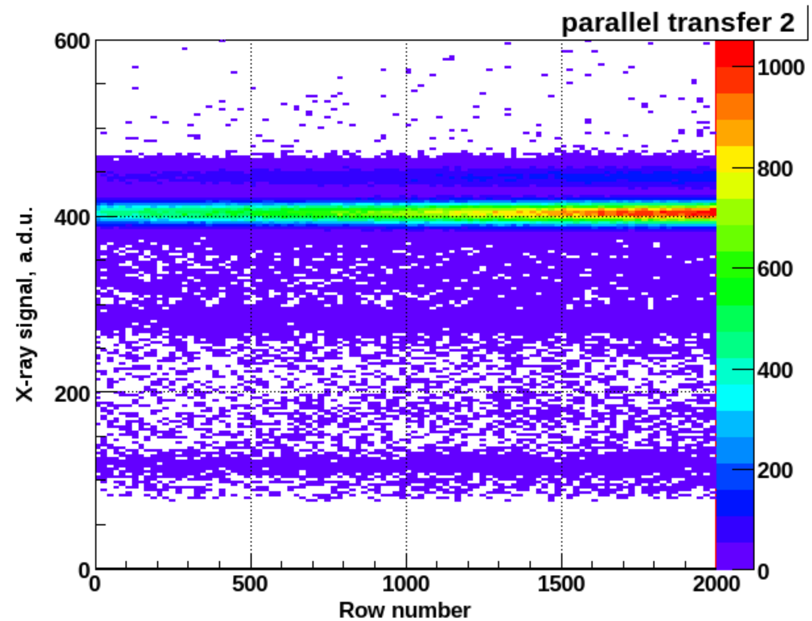

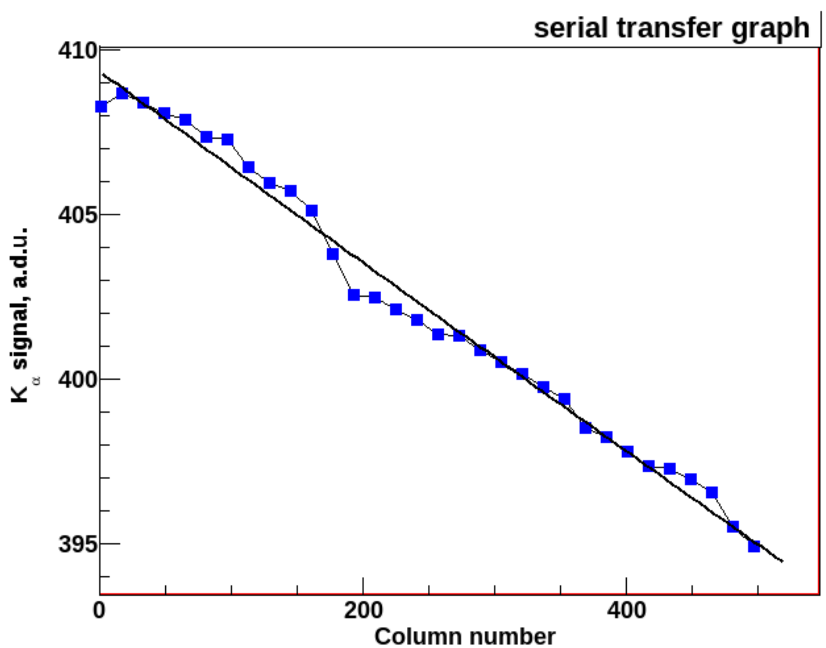

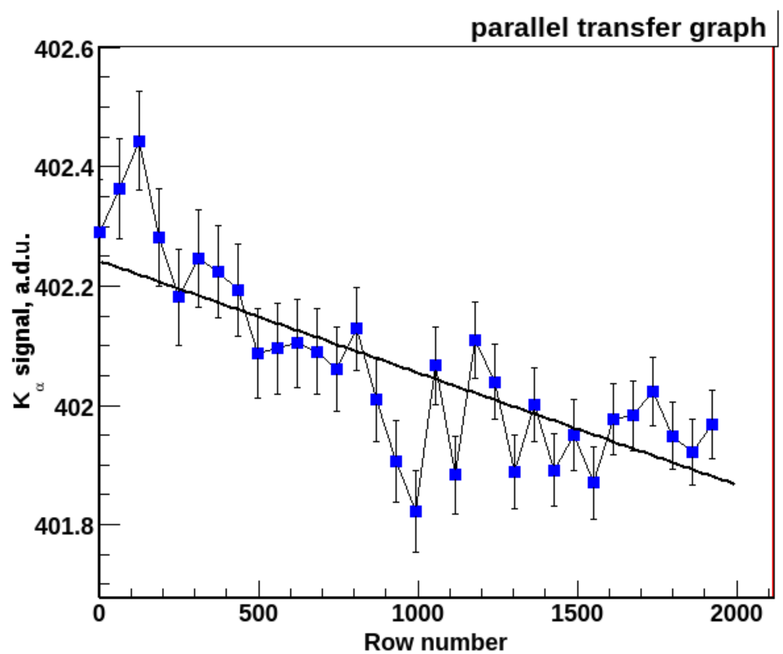

CTE measurements with X-rays. Average cluster. T=-150C

Average cluster profile , e-, close to readout node, 125 transfers on average.

y/x	0	1	2	Δ(right-left)
0	25.4 +/- 0.1	152.2 +/- 0.35	29.7 +/- 0.1	
1	151.3 +/- 0.35	879.9 +/- 0.45	156.7 +/- 0.35	5.4 +/- 0.5
2	25.6 +/- 0.1	152.6 +/- 0.35	29.7 +/- 0.1	

Average cluster profile, e-, away from readout node, 375 transfers on average.

y/x	0	1	2	Δ(right-left)
0	22.5 +/- 0.1	146.9 +/- 0.36	31.5 +/- 0.1	
1	144.6 +/- 0.36	871.1 +/- 0.46	161.0 +/- 0.35	16.4 +/- 0.5
2	22.7 +/- 0.1	147.2 +/- 0.36	31.7 +/- 0.1	

Using the number of electrons in the central pixel one can calculate CTE in extended pixel response, EPER, style. This calculation gives CTE =0.99981 and CTI=1.9 10-5.
EPER approach underestimates CTI by more than factor of 3 compare to the aperture method. This is not surprising because EPER method does not take into account the release time of trapped charges.

Defect diagnostics using X-rays

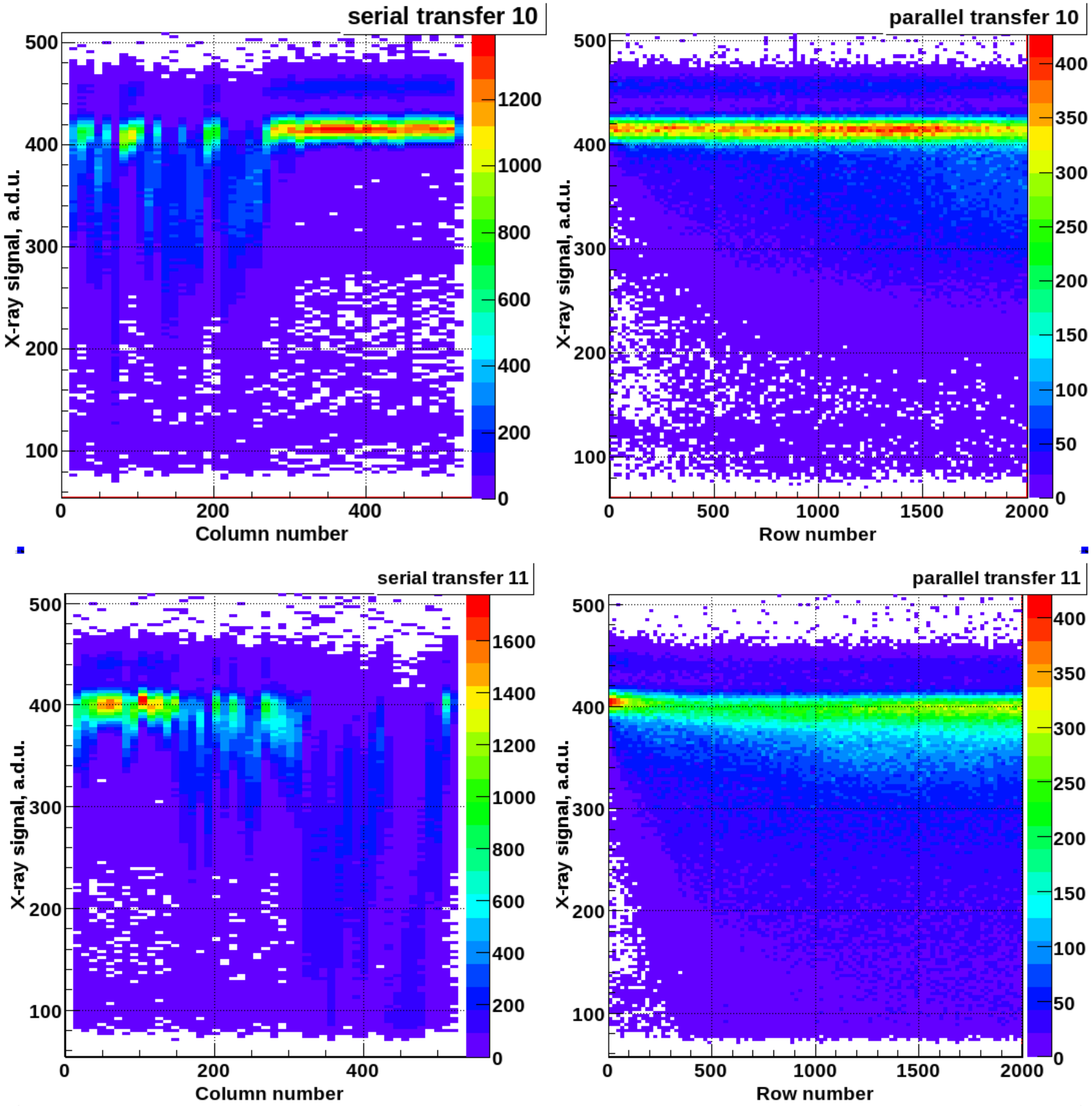

Defect diagnostics using X-rays (location)

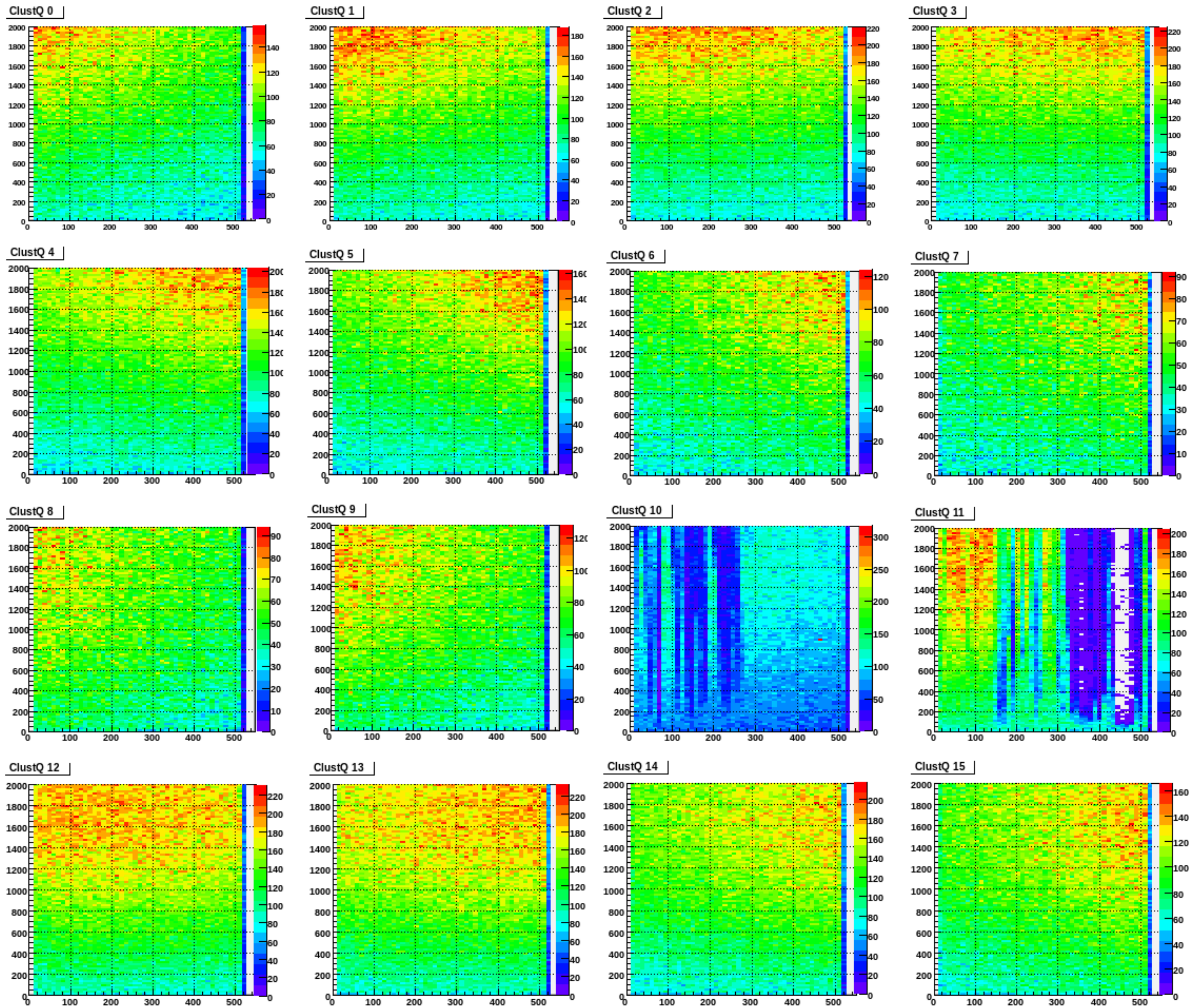

CONCLUSIONS

- it is demonstrated that X-rays analysis is the powerful tool for CCD characterization
- X-rays very useful for sensor PSF characterization
  - for CCDs with small pixel sizes
  - low read-out noise
- X-rays can be used for CTE measurements
  - provide practical and robust measurements
  - achieve required level of accuracy
- X-ray analysis reveals and pinpoints defect sites.

POCKET PUMPED IMAGE ANALYSIS

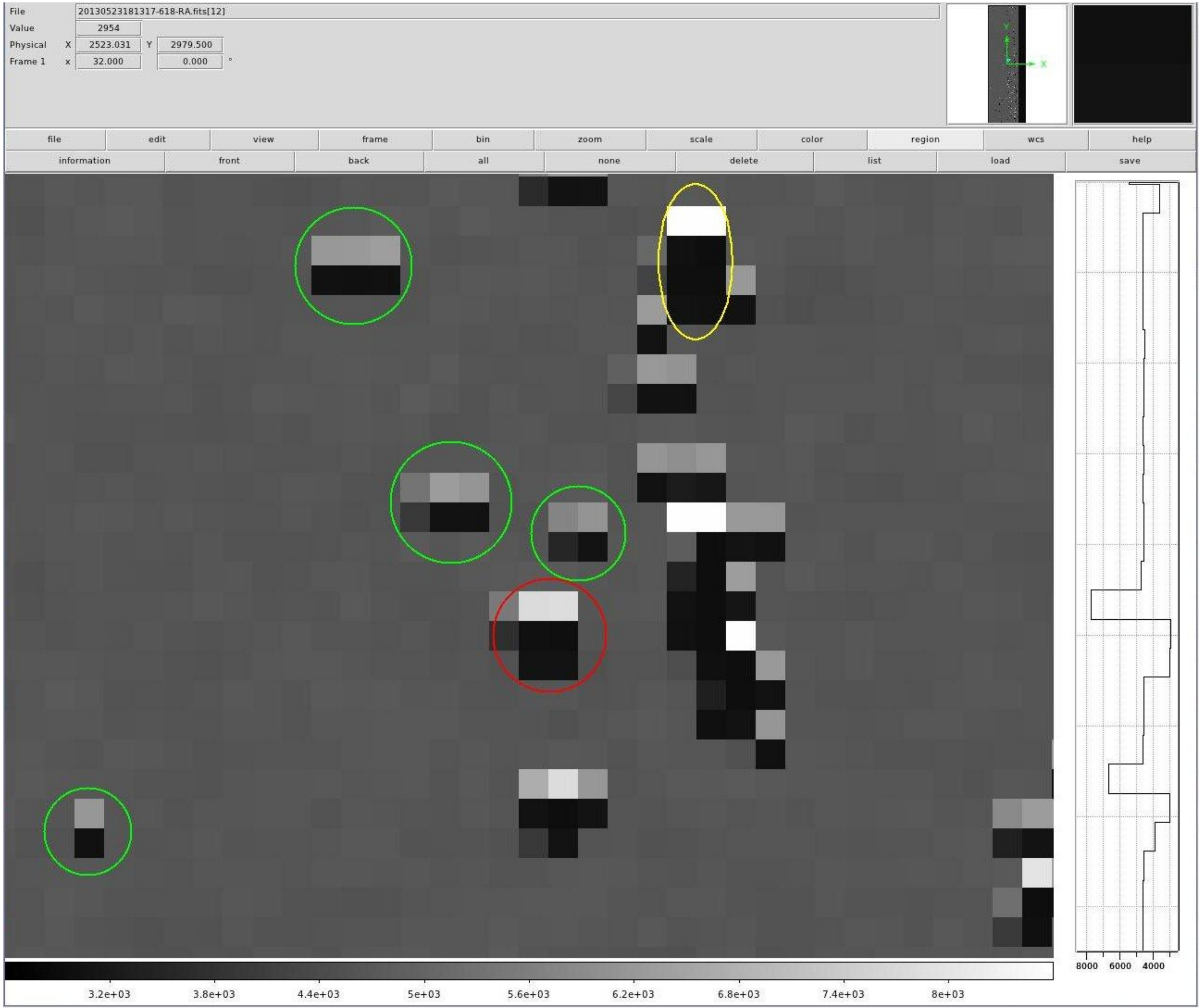

Trap identification. Amplitude distribution

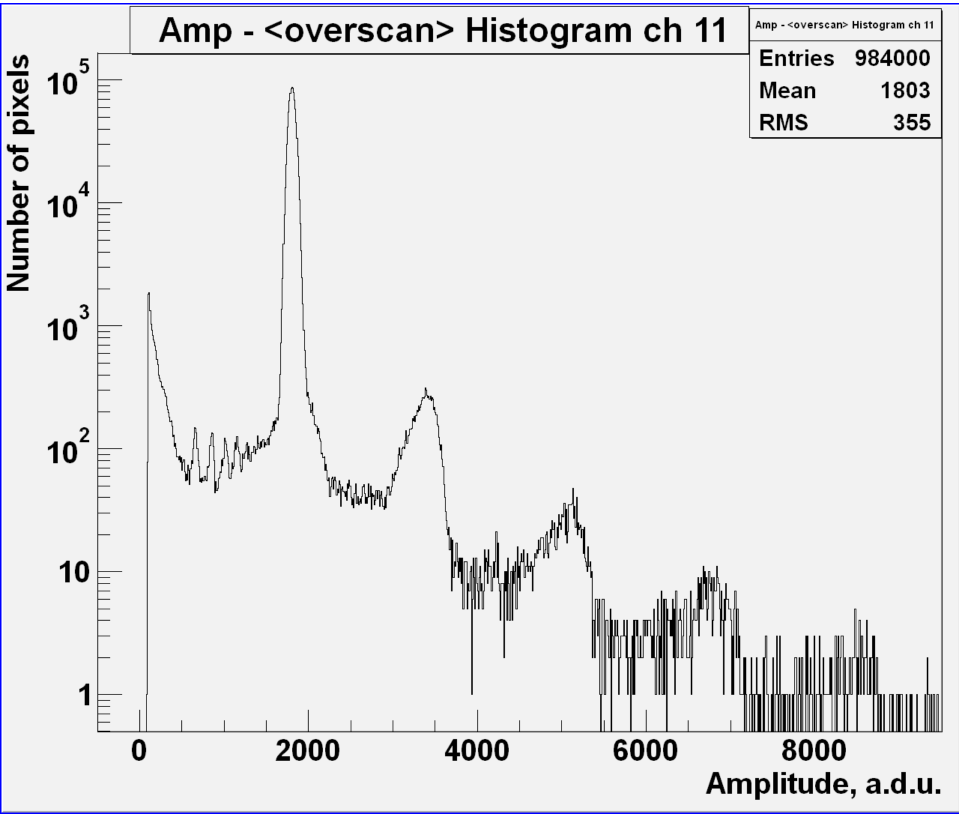

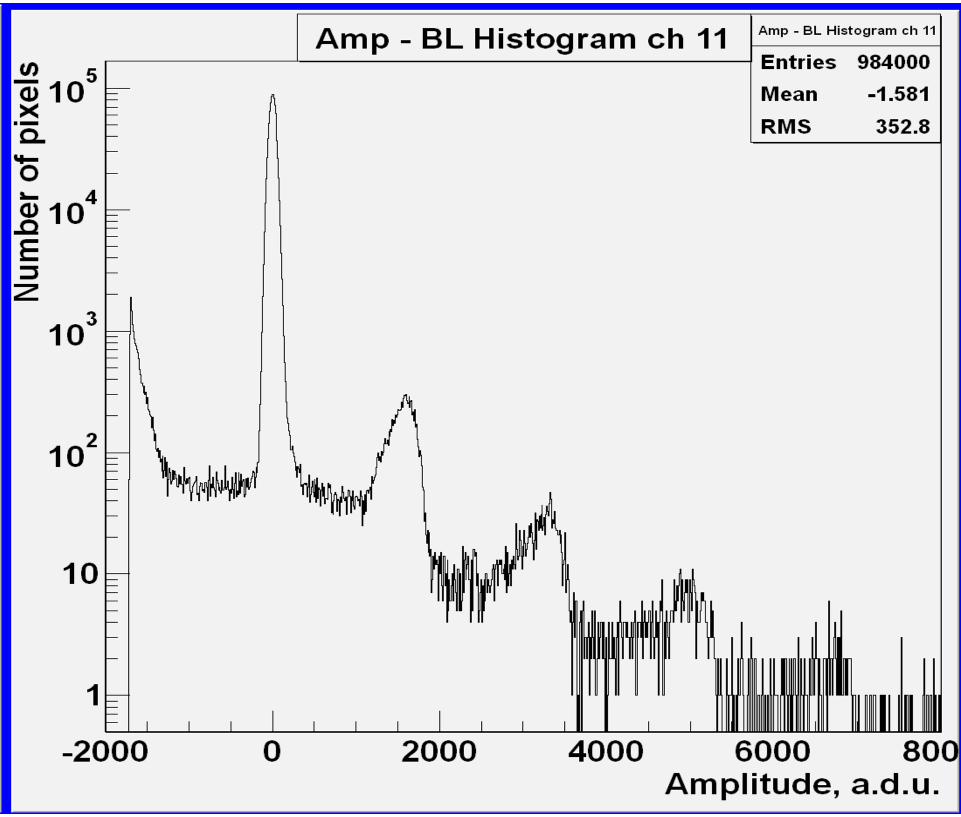

Trap identification. Amplitude-Amplitude plot

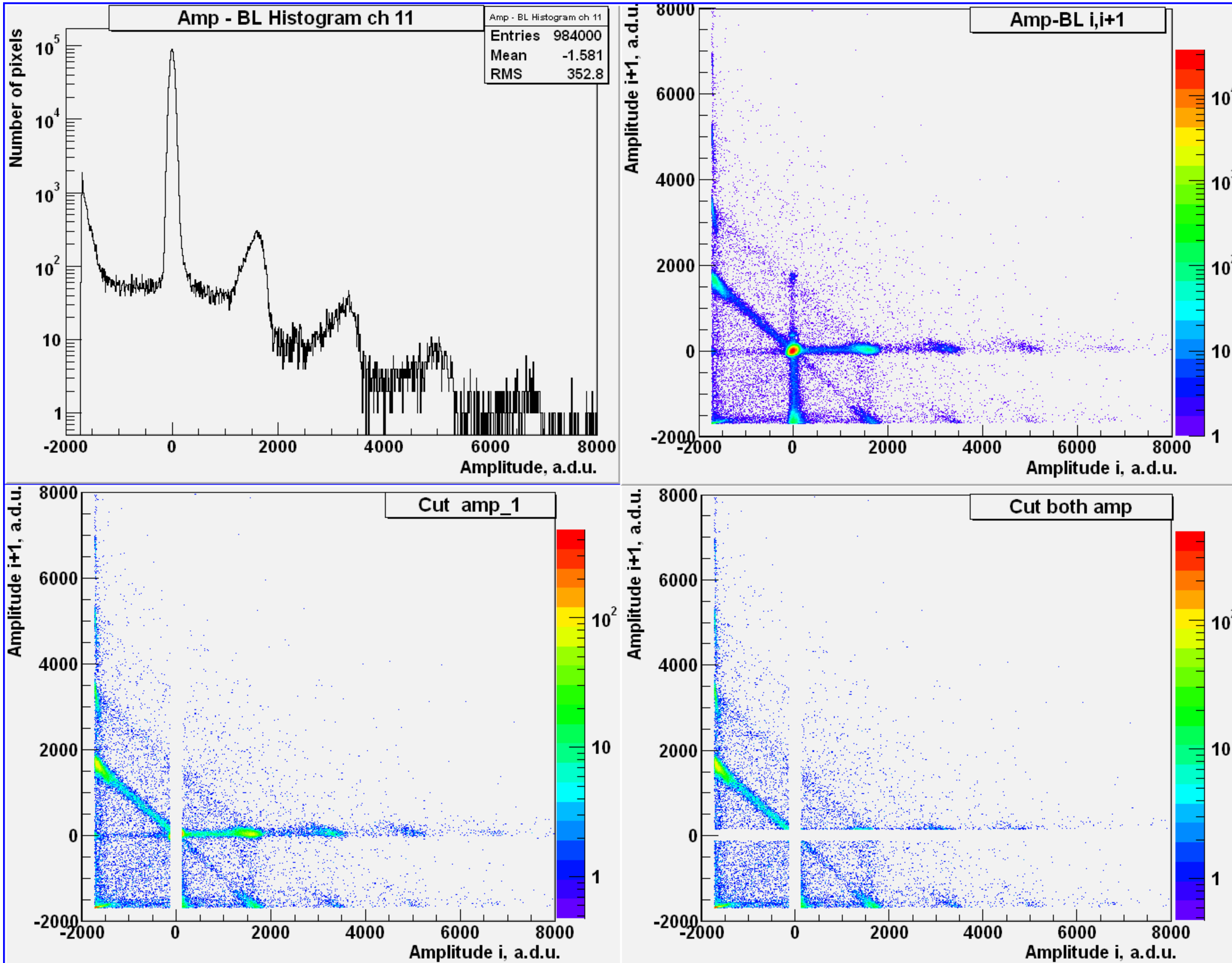

Trap identification. Amplitude-Amplitude plot

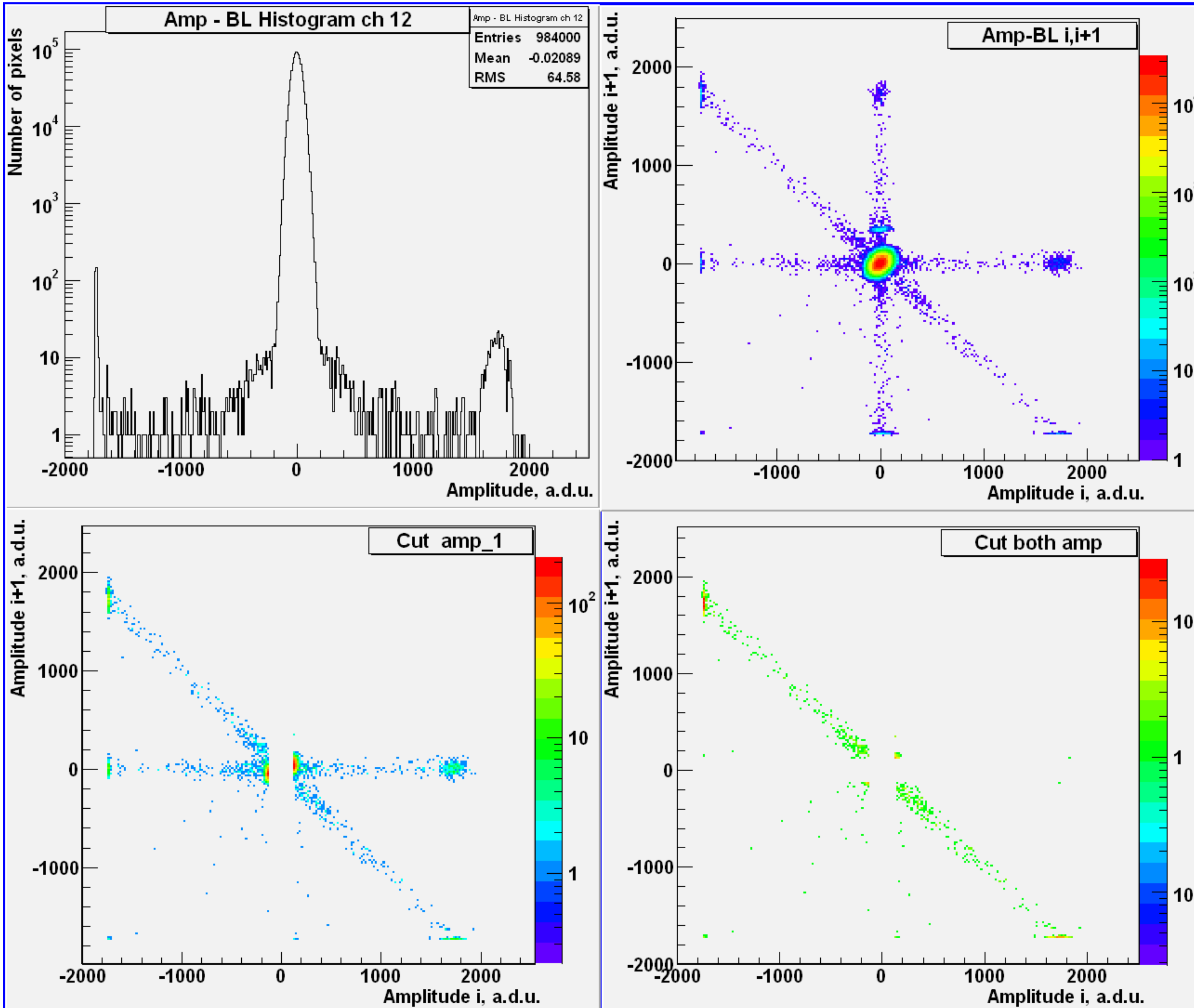

Trap identification. Correlator

$$C_2 = \frac{amp_i}{\sigma} * \frac{amp_{i+1}}{\sigma}$$

the parabolic shape is expected for amplitude dependence since amount of charge lost in one pixel is equal to amount of charge gained by another pixel and $C_2 \sim -amp^2$

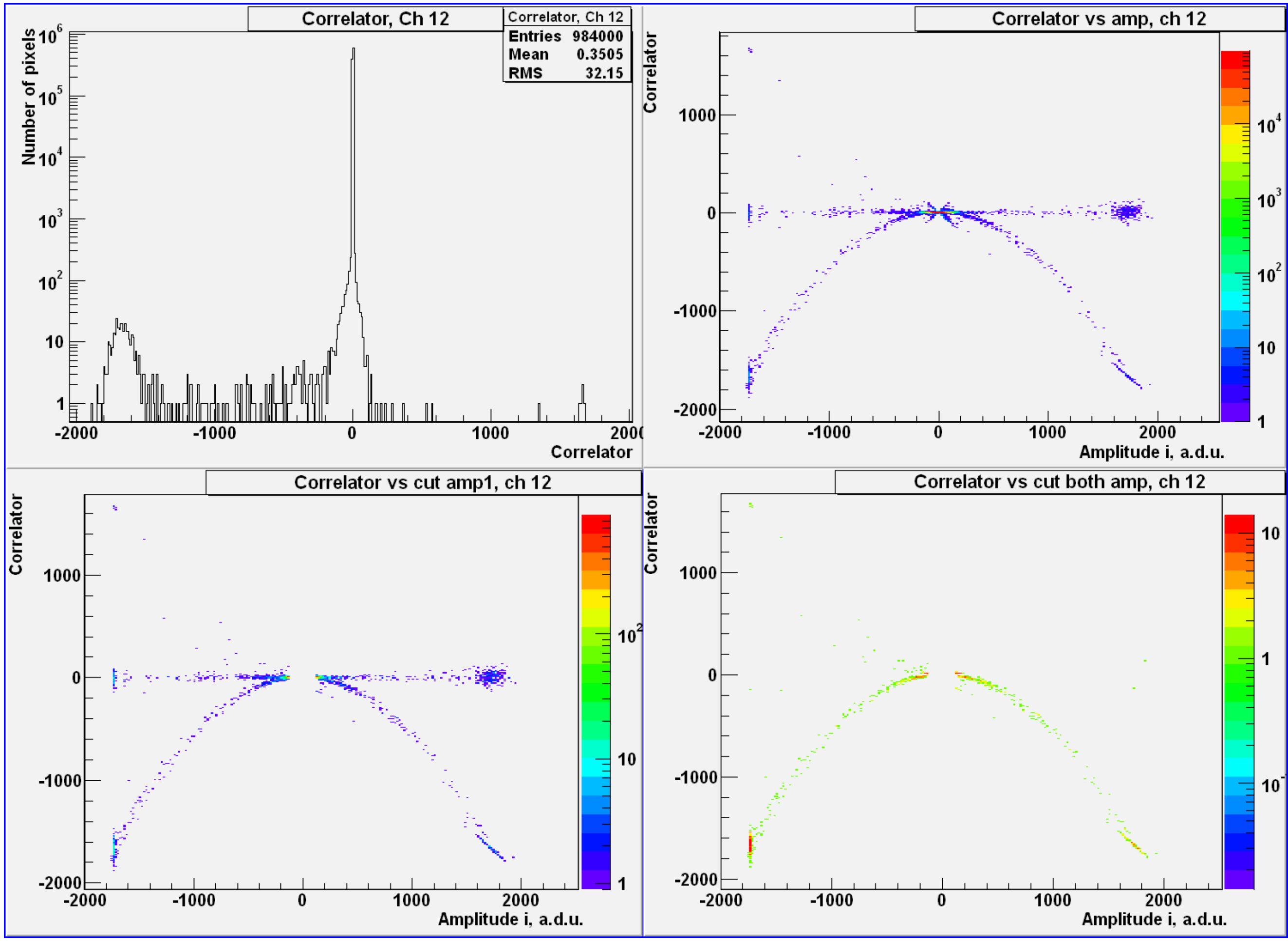

Trap count

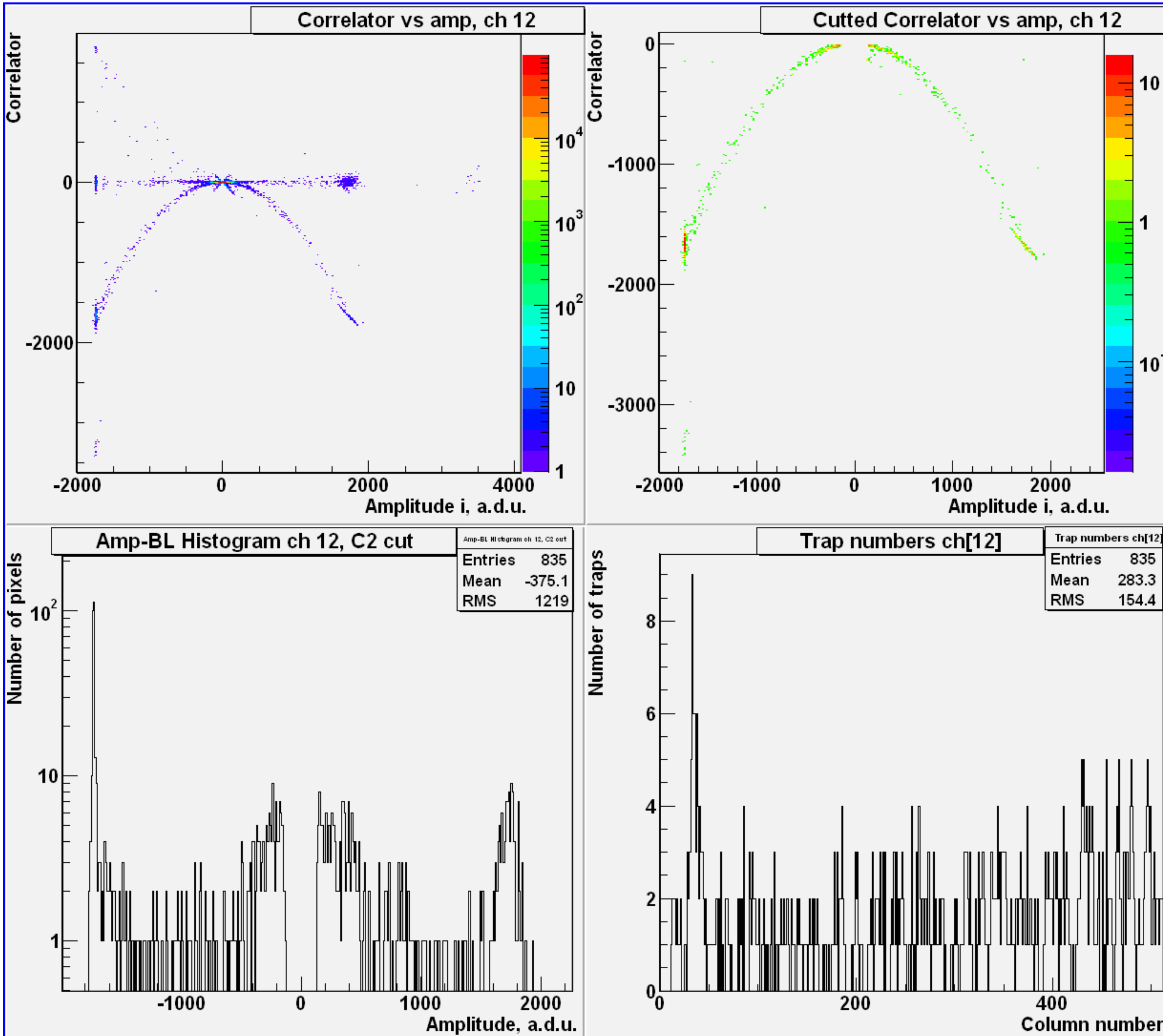

Correlator vs amp, ch 12
Correlator
Amplitude i, a.d.u.
Cutted Correlator vs amp, ch 12
Correlator
Amplitude i, a.d.u.
Amp-BL Histogram ch 12, C2 cut
Amp-BL Histogram ch 12, C2 cut
Entries 835
Mean -375.1
RMS 1219
Number of pixels
Amplitude, a.d.u.
Trap numbers ch[12]
Trap numbers ch[12]
Entries 835
Mean 283.3
RMS 154.4
Number of traps
Column number

Trap count

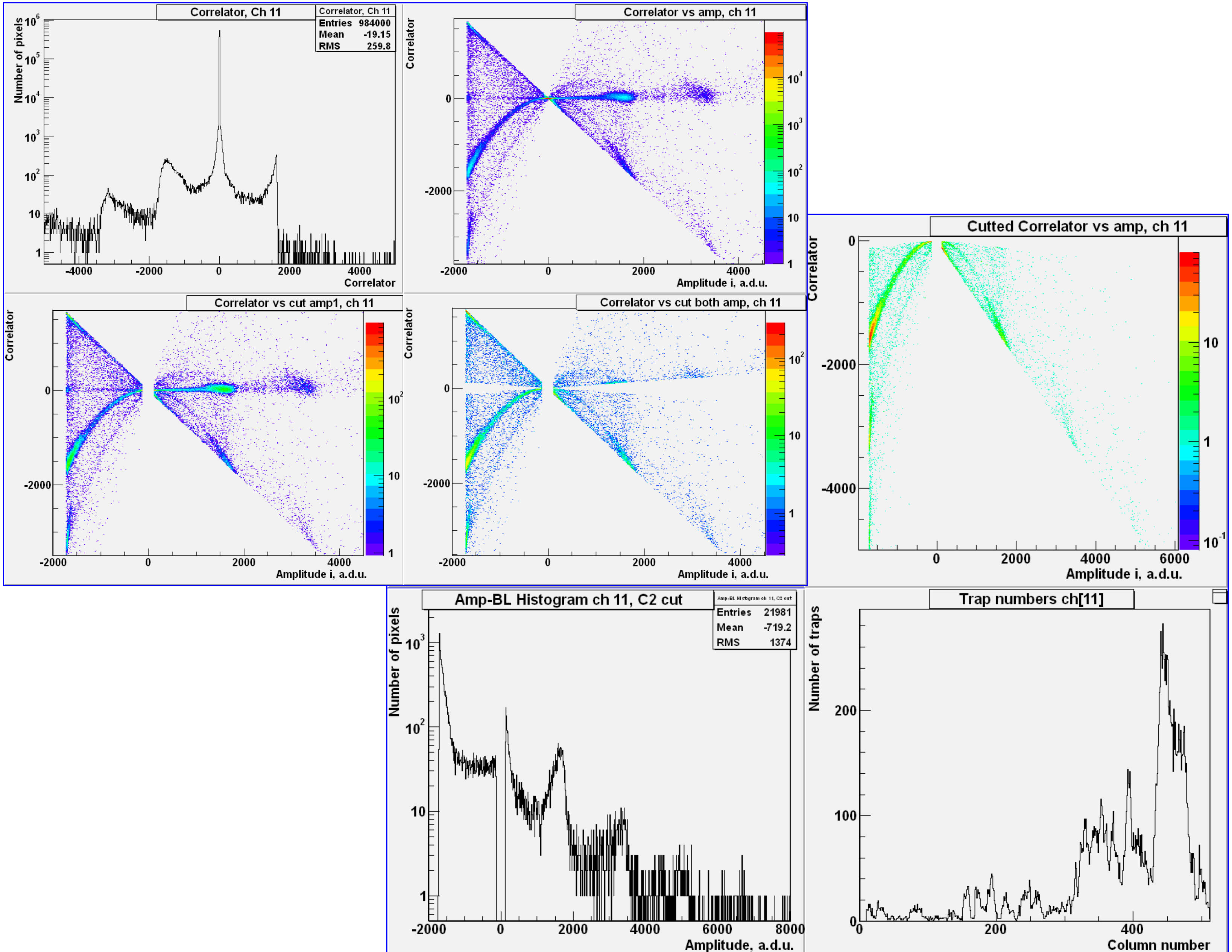
Correlator, Ch 11
Correlator, Ch 11
Entries 984000
Mean -19.15
RMS 259.8
Number of pixels
Correlator
Correlator vs amp, ch 11
Correlator
Amplitude i, a.d.u.
Cutted Correlator vs amp, ch 11
Correlator
Amplitude i, a.d.u.
Correlator vs cut amp1, ch 11
Correlator
Amplitude i, a.d.u.
Correlator vs cut both amp, ch 11
Correlator
Amplitude i, a.d.u.
Amp-BL Histogram ch 11, C2 cut
Entries 21981
Mean -719.2
RMS 1374
Number of pixels
Amplitude, a.d.u.
Trap numbers ch[11]
Number of traps
Column number

POCKET PUMPED IMAGE. CONCLUSION

Trap identification technique has been developed.
This technique works on pocket pumped images.

- traps can be counted in individual columns, rows etc
- trap location can be reported as well, for example, trap map can be generated

Full simulations: model & equations

- electrons generated by X-ray drift from point of generation x_0 to the gates
- electrons diffuse with characteristic sigma $\sigma(t)$

$$\sigma^2(\mathrm{t}) = 2\mathrm{Dt},\ \mathrm{D\text{ - is diffusivity}}$$

$$\sigma^2(\mathrm{t}) = \sigma^2_{\max} \cdot \frac{t}{t_{\max}}$$

- drift time is calculated as

$$\mathrm{t} = \int_{x_0}^{d} \frac{dx}{\mathrm{v}(x)}$$

$$\mathrm{v}(E) = \frac{\mu E}{1 + \mu E / \mathrm{v}_s}, \quad \mu - \text{electron mobility}$$

$\mathrm{v_s}$ - saturation velocity

$$\mathrm{E(x)} = -\left[\frac{V_{op} - V_d}{d} + 2\frac{x}{d} \cdot \frac{V_d}{d} \cdot \frac{1}{C_j}\right], V_{op} - \text{applied voltage,}$$

V_d - depletion voltage, C_j - factor taking into account the pn- junction

Full simulations: output plots

Diffusion sigma maximum is at the window

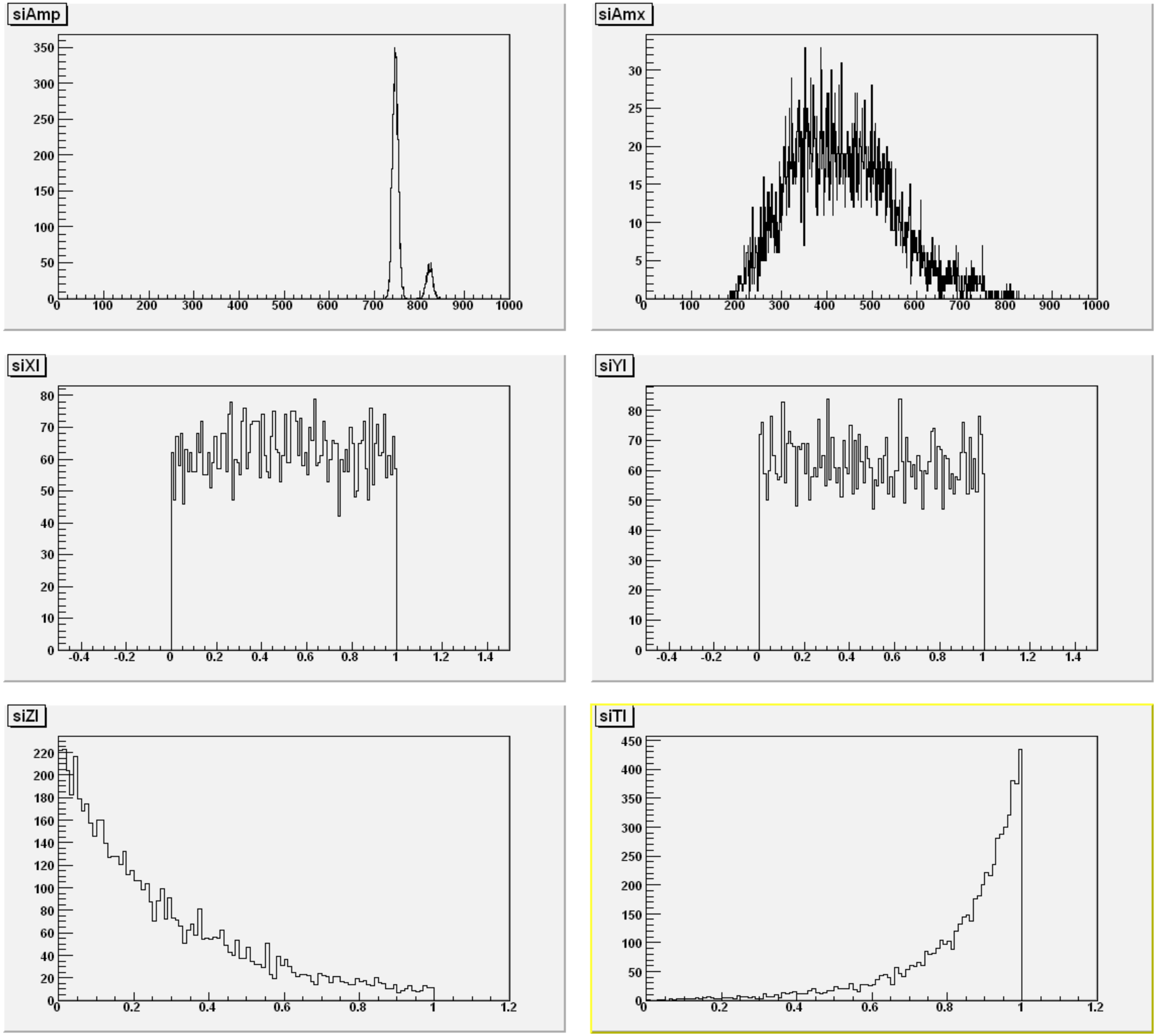

Transformations

The selection of trap bands in the amplitude scatter plot can be simplified using coordinate system transformation.
The useful transformation is rotation by 45 degree

$$A+ = (amp_i + amp_{i+1})/\sqrt{2}$$

$$A- = (amp_{i+1} - amp_i)/\sqrt{2}$$

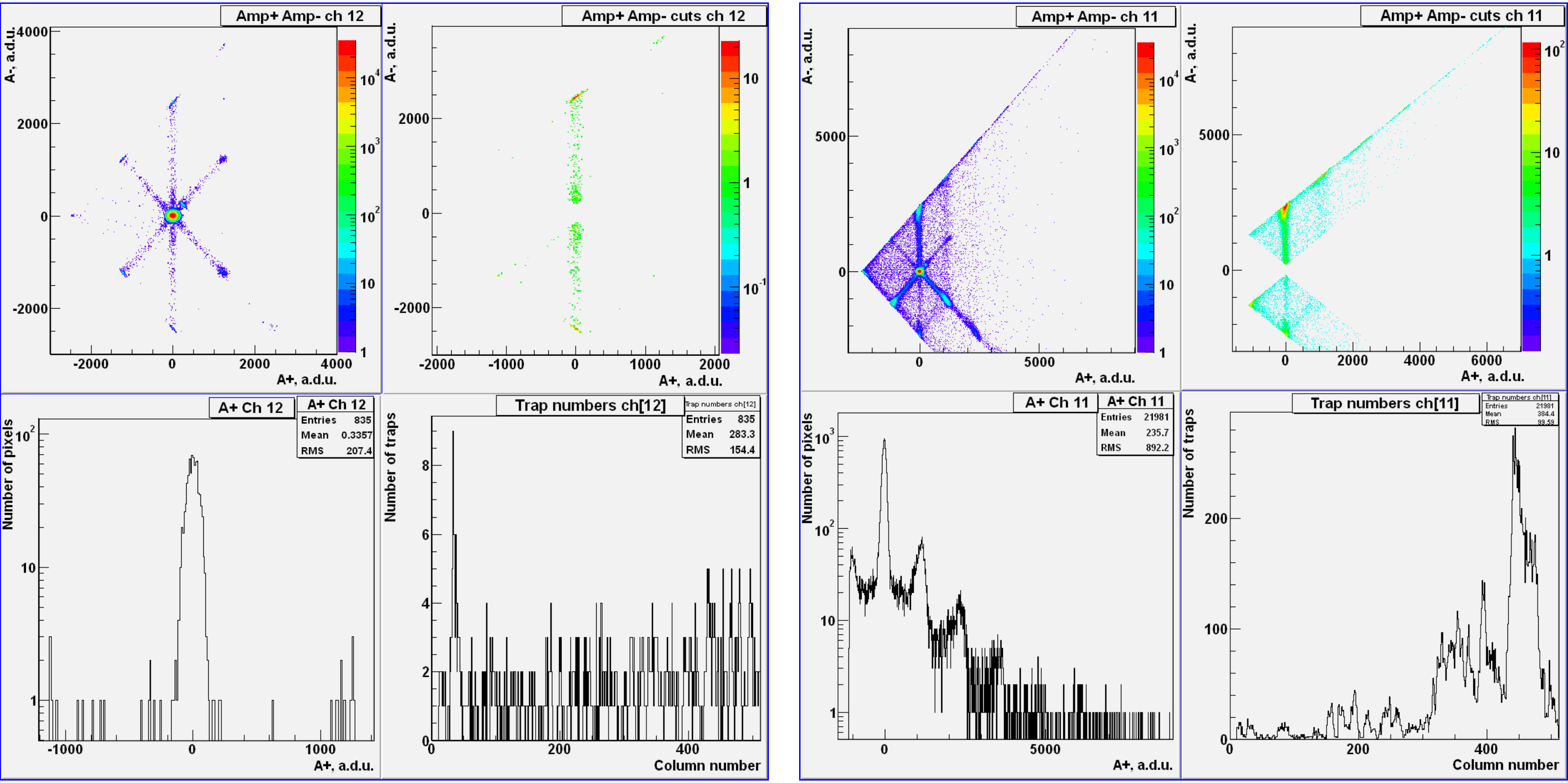

The Wallet Card

- Three Mirror Anastigmat (TMA) optical design.
    - 8.4 meter primary, 6.5 meter effective aperture
    - 3.4 meter diameter secondary
    - 5 m tertiary is being fabricated in same substrate as primary mirror
    - three-element refractive corrector
    - f/1.2 beam delivered to camera
    - 9.6 square degree field (on science imaging pixels)
    - optics deliver < 0.2 arcsec FWHM spot diagram,
    - 6 filters: ugrizy: 320 nm to 1050 nm (UV atmospheric cutoff to Si bandgap)

- 3.0 Gpixel camera
    - 10 micron pixels, 0.2 arcsec/pixel
    - Deep depletion (100 μm), high-resistivity CCDs for NIR response
    - Dual 15 second exposures (to avoid trailing of solar system objects)
        - 2 second readout (trade between noise and imaging efficiency)
        - 550 kpix/sec through 16 amps/CCD x 189 CCDs = 3024 channels
        - 12 GBytes per image (as floating point numbers), 20 TBytes/night.

- Real-time frame subtraction for time domain alerts, ~850 visits for each patch of sky, allows co-adds to r ~ 27 (AB), over 18,000 square degrees.

Camera

- 3.2 Gigapixels
- 0.2 arcsec pixels
- 9.6 square degree FOV
- 2 second readout
- 6 filters

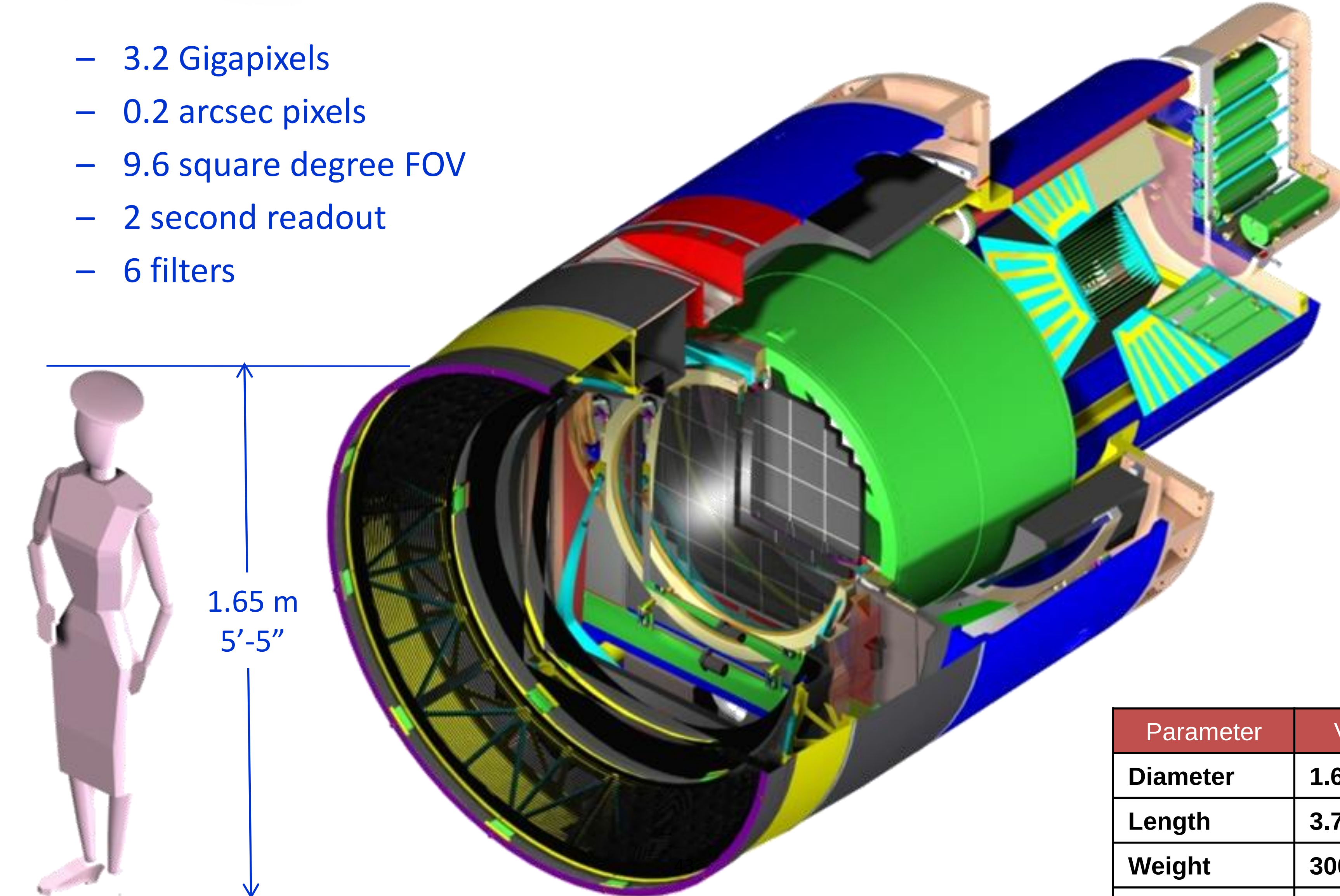

Parameter	Value
Diameter	**1.65 m**
Length	**3.7 m**
Weight	**3000 kg**
F.P. Diam	**634 mm**

Primary/Tertiary in Fabrication, completion in 2014

44